Assaying Dopamine with Saccharide Carbon Dots

By

Peter Ogunsanya

A Thesis submitted in Partial Fulfilment of the requirement for the Degree of Master of Science in Chemistry

Middle Tennessee State University

December 2023

Thesis Committee:

Dr. Charles Chusuei

Dr. Ngee Sing Chong

Dr. Chengshan Wang

ACKNOWLEDGMENTS

I would like to express my sincere gratitude and immense respect from my heart to my research advisor Dr. Charles C. Chusuei for his generous support towards me throughout my research work.

I also would like to thank Dr. Ngee Sing Chong and Dr. Chengshan Wang who are my research committee members for their valuable time and reading and comments on my thesis work.

My sincere thanks to Dr. Joyce Miller for giving me time and helping with the Scanning Electron microscope. I am also grateful to Dr. Leblanc and his team from the Department of Chemistry, University of Miami, Florida for helping with the synthesis of carbon dots used in my research work.

I am also grateful to the Department of Chemistry for providing me with an opportunity to pursue my master's degree from MTSU. I am also grateful to the department for providing chemicals, research labs, materials, and instruments to carry out the research experiments.

I am also thankful to my research team members, Ram, Sidney, and Morgan, for their help and cooperation throughout the experiments.

ABSTRACT

Dopamine, also known as 4-(2-aminoethyl) benzene-1,2-diol (DA), is a neurotransmitter produced by brain neurons. It serves a crucial role in transmitting neurological signals. Dopamine exerts a substantial influence on various physiological systems in the human body, including the metabolism, central neurological system, renal system, and hormonal system.[1] Insufficient levels of dopamine can lead to many neurological disorders, such as Parkinson's disease and schizophrenia, and a high level of dopamine excretion is a biomarker for the electrochemical detection of DA. This work explores the deposition of Saccharide carbon dots (namely lactose, glucose, and galactose) onto the surface of a glassy carbon electrode. This is followed by the deposition of a 2 wt% Nafion solution. The purpose of this process is to detect dopamine within two concentration ranges: 0.01mM – 0.1mM and 0.1mM – 1Mm. Cyclic voltammetry was employed to measure the relationship between current and concentration. At a concentration of 1mM, the lactose carbon dot exhibits the highest oxidation peak height, followed by glucose and then galactose. Studies on the selectivity between dopamine and the two other analytes—d-glucose and uric acid—that could obstruct neuroblastoma screening mechanisms during excretion were conducted. The results indicate that lactose CDs' reaction to GCE was largely selective for dopamine at the oxidation potential, with little to no response to either of the other analytes. The average size of the carbon dots, with a diameter of (156 ± 7) nm, was determined using scanning electron microscopy. This result provides an understanding of the uniformity of the carbon dots, with a diameter greater than the average size of carbon dots (>10nm), this also explains the discrepancy between the Raman results from Chusuei et al. and the behavior of carbon dots.[2]

TABLE OF CONTENTS

PAGE

LIST OF FIGURES

FIGURE **PAGE**

LIST OF TABLES

TABLES **PAGE**

CHAPTER 1

INTRODUCTION

Allotropes refer to distinct forms of an element that exist in the same physical state (solid, liquid, or gas) and exhibit varying physical and occasionally chemical characteristics. They display a wide spectrum of physical and chemical properties because of their complex structures and chemical relationships. Carbon is particularly fascinating among the several allotropic elements because of its extensive array of practical uses.[1] Carbon nanoparticles are 100,000 times smaller than human hair and have diameters of less than 100 nm. [2].

The use of carbon nanomaterials as sensors, electrodes, supercapacitors, batteries, and electronics has been made possible by features like as electrochemical activity, conductivity, surface area, and ease of functionalization [3]. Carbon nanomaterials are can be categorized as carbon nanotubes, which are one dimensional nanomaterials that consist of sp_2 hybridized carbon. Additionally, it is divided into single and multi-wall carbon nanotubes. Single-walled CNTs are formed of a single cylindrical graphene sheet with hemi fullerene caps covering the ends. While multiwalled CNTs are more complex than single-walled ones, tubes are stacked over one another successively with an increase in diameter. [4] Graphene is a nanomaterial consisting of sp_2 carbon atoms organized in a two-dimensional honeycomb lattice structure. It is acknowledged for its ability to transfer electrons, conductive properties, expansive surface area, and compatibility with living organisms.[5]

CARBON DOTS

The initial study on the synthesis of carbon dots revealed the serendipitous identification of luminous carbon nanoparticles by an unconventional manufacturing method. The particles were a secondary result of the production of carbon nanotubes through the synthesis of arc-discharged soot.[6] During the purification process of single-walled carbon nanotubes (SWCNTs), two primary impurities were separated and examined. It was discovered that fluorescent carbon impurities have remarkable size-dependent emissive capabilities, which, upon surface functionalization, were increased even more.[7] Carbon-dot production was thought to occur through the fragmentation of carbon nanotubes, aided by electrolyte molecules entering "defect areas" on the nanotubes' surface.

The CDs are nanoscale particles that are predominantly spherical in shape, with diameters smaller than 10 nm. They consist of a carbon core that is often surface-functionalized and contains sp_2 and sp_3 hybridized carbon entities. These carbon entities facilitate various interactions with neighboring molecules and electromagnetic waves.[8] A system with such low dimensions exhibits quantum confinement along with unique properties as enhanced band gap and quantum yields, photostability, quantum size effects, better water solubility, biocompatibility, and non-toxicity.[9]

The simplicity of synthesis, cost-effectiveness, and safety of CDs as nano-catalysts are particularly appealing. These factors, along with their great solubility in water, may enable their application even in biological or quasi-biological conditions [10]. The surface features and potential applications of carbon dots exhibit significant variation, contingent upon the precursor chemicals and synthesis methodologies employed. CDs possess a strong attraction to the receptors of their precursor molecules in biological systems, rendering them well-suited as substitutes for targeted drug delivery methods.[11]

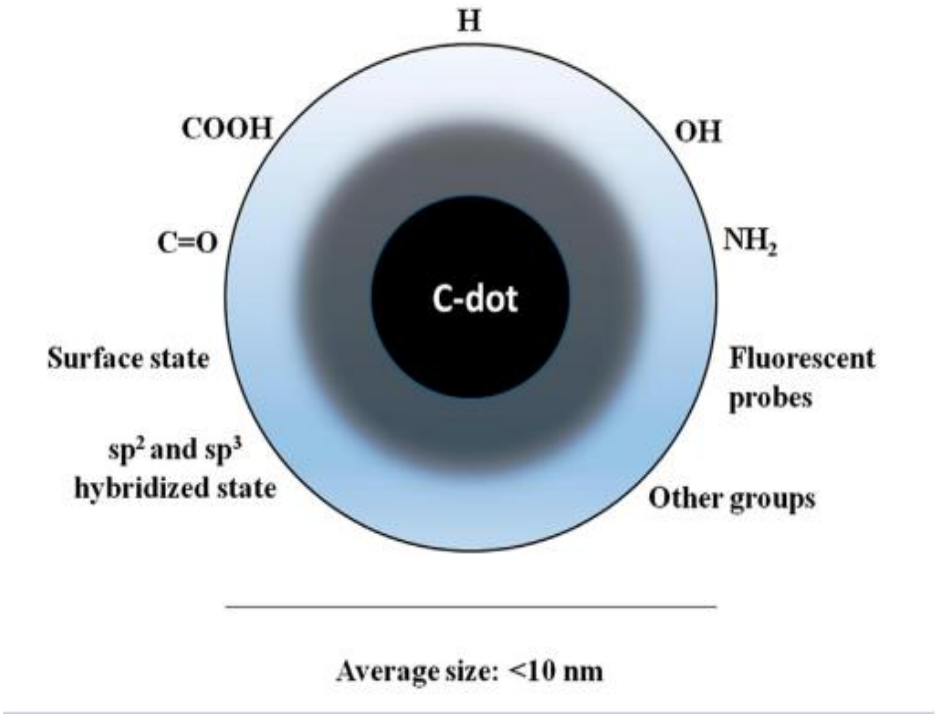

Fig 1: Image showing the structure of CDs [11]

SYNTHESIS OF CARBON DOTS

Gaining knowledge about the manufacturing, composition, and characteristics of nanomaterials is the initial stage in manipulating them for applications. Carbon dots have been generated by two separate procedures known as top-down and bottom-up synthesis. The top-down technique entails the transformation of bigger precursor molecules, often graphite, into CDs. This approach commonly employs laser ablation, arc discharge, and electrochemical approaches.[12] On the other hand, bottom-up approaches involve simpler molecular precursors polymerized into CDs. Solvothermal and microwave synthesis, high thermal decomposition, and hydrothermal carbonization are a few bottom-up strategies. [13]

The various synthesis methods for carbon dots are depicted below:

Top-down synthesis

The top-down approach involves the conversion of massive precursors into nanoparticles, namely CDs, using physical, chemical, or electrical means. Considerable research utilizing top-down methodologies first concentrated on bigger carbon-based materials, such as carbon nanotubes (CNTs) or graphite.[14] The following sections outline several frequently used top-down methodologies:

Laser Ablation

Laser ablation is the technique of aiming a laser at a solid target that is enclosed by a surrounding material. This process leads to the elimination and transformation of surface atoms, together with the interaction of energetic atoms and molecules within the medium. As a result, a plasma plume consisting of ions, electrons, and high-energy particles is created.[15] The production of CDs is influenced by the properties of the desired outcome and the material being utilized, together with the specifications of the laser employed, including its wavelength, fluence, pulse duration, and intensity. This feature allows users great flexibility in designing customized CDs.[16] The utilization of a low-pressure vapor medium is advantageous as it facilitates the generation of smaller nanoparticles while minimizing the likelihood of aggregation. In addition, laser ablation allows for the creation of specific carbon allotropes and nanocrystal structures.[16]

Compared to hydrothermal approaches, laser ablation has the advantage of synthesizing CDs in a relatively short period of time (1 ms) and a higher likelihood of obtaining intrinsically bright

CDs.[17] Nevertheless, there are still obstacles to overcome in effectively controlling the range of particle sizes and crystal structures. Additionally, there are considerable energy demands and post-processing necessities that may potentially diminish the overall production output.[15]

Arc discharge

Arc discharge is a commonly employed technique for producing a wide range of carbon nanostructures, such as multi-walled carbon nanotubes, carbon nano-onions, and few-layer graphene. Various investigations have established the usefulness of carbon dots in their synthesis. Carbon quantum dots were produced using a process of submerging arc discharge in water. The process entailed creating an electric discharge by connecting and positioning two graphite electrodes in distilled water, maintaining a tiny distance between them.[18]

Three distinct products were identified: a solid substance consisting of CNOs and MWCNTs, a mixture of floating materials containing CNOs and MWCNTs, and a liquid suspension enriched with CDs and graphene oxide that may be subsequently filtered. Consequently, the synthesis and functionalization processes might be interconnected. The drawbacks of this technology encompass difficulties in separating the many types of nanostructures produced, substantial energy requirements, and the necessity for specialized equipment.[19]

Electrochemical methods

Electrochemical methods involve producing carbon dots (CDs) by applying voltage to a solution containing electrodes. Solutions are often supplemented with electrolytes to enhance their conductivity. Solutions are often supplemented with electrolytes to enhance conductivity.[20] An effective method is electrochemical exfoliation, which utilizes graphite and NaCl as electrodes and

electrolytes. An electric field induced the formation of hydroxyl ions from water, subsequently leading to the oxidation of the graphite anode. The presence of anions in the solution led to intercalation and exfoliation, leading to the formation of carbon nanosheets. Their breakdown into carbon dots was facilitated by a magnetic stirring mechanism.[21]

Electrochemical procedures are frequently employed because they offer consistent results, have the potential for large-scale manufacturing, need simple equipment and maintenance, and provide a broader range of precursor options[20].

Bottom-up synthesis

In recent years, bottom-up approaches for synthesizing CDs from smaller molecules have gained popularity due to their environmental simplicity, ability to incorporate multiple readily available natural molecules, simplicity and cost-effectiveness, ease of functionalization, and enhanced flexibility and control. This has facilitated the development of clearly defined CDs tailored to certain purposes. [22]

The predominant methods utilized are solvothermal, hydrothermal, and microwave synthesis.

Solvothermal synthesis

In recent years, bottom-up approaches for synthesizing CDs from smaller molecules have gained popularity due to their environmentally friendly characteristics, utilization of multiple easily accessible natural molecules, simplicity and cost-effectiveness, ease of functionalization, and enhanced flexibility and control. This has enabled the development of precisely defined CDs customized for certain uses. After synthesis, the CDs undergo several purification procedures,

such as washing, centrifugation, and drying.[23] The size and morphology of CDs can be effectively regulated by manipulating the temperature and pressure during solvothermal synthesis.

However, when this technology is applied on a wider scale, issues related to the transfer of heat become apparent. Conventionally, the reaction vessel is heated through conduction. To enhance the effectiveness of solvothermal synthesis, it is necessary to maintain elevated internal pressure and temperature inside the autoclave, resulting in the solvent reaching a state of supercritical fluidity.[24]

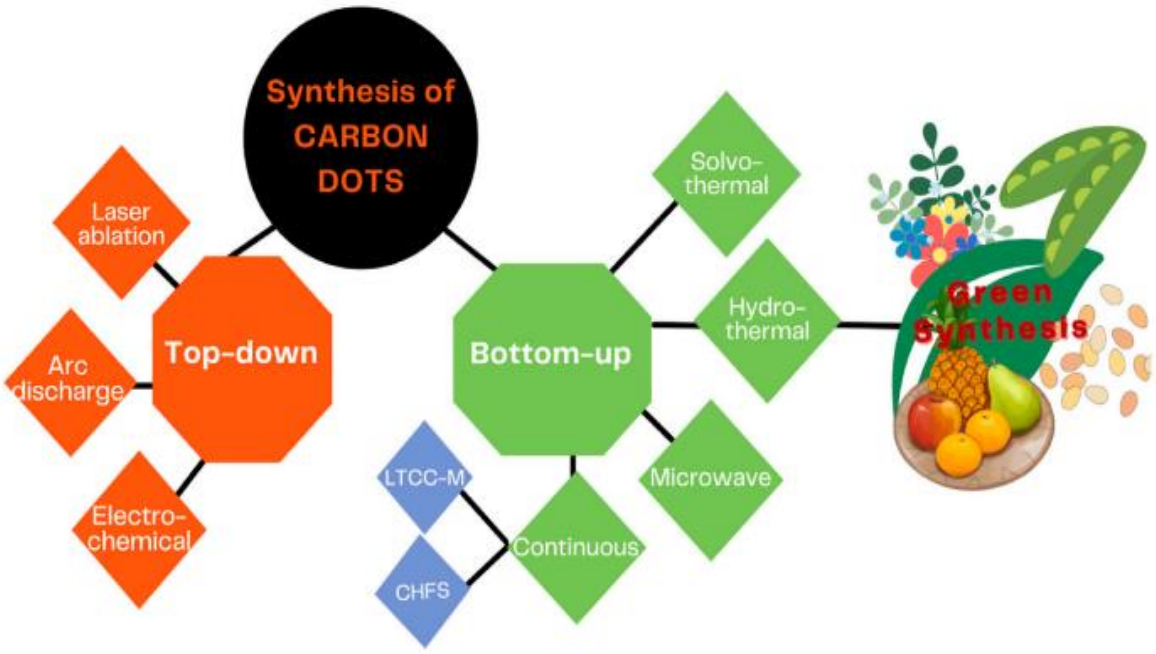

Fig. 2: Various synthesis methods of carbon dots.[25]

Hydrothermal synthesis

Hydrothermal synthesis has been extensively utilized to produce carbon dots. The size of carbon dots is typically controlled by adjusting precursor quantities, processing temperatures, and reaction periods. [26] While carbonization and polymerization significantly influence the average size of carbon dots, these processes cannot be directly observed within the black box/hydrothermal reactor.[27]

The sizes of carbon dots derived from the hydrothermal treatment of sucrose precursor were notably influenced by the decomposition and polymerization processes, as explained.[28] During the process of decomposition, the sucrose molecules in a water solution undergo hydrolysis, leading to the creation of fructose and glucose. Subsequently, these molecules undergo further degradation into smaller organic entities, including furfurals and weak acids.[29] Following that, these organic compounds undergo the process of polymerization, leading to the formation of larger molecules that ultimately give birth to the production of the CQDs within the hydrothermal reactor.[30]

Hydrothermal synthesis is a type of solvothermal synthesis that uses distilled water as the solvent and produces powder-like, extremely crystalline nanoparticles. A combination of precursors is placed into a stainless-steel autoclave walled with Teflon, just like in solvothermal synthesis.[31]

Hydrothermal synthesis has the disadvantage of having poorer yields and longer reaction periods than co-precipitation techniques. Homogeneous heat transfer and pressure maintenance within reaction vessels, like the solvothermal technique, create obstacles in scaled-up synthesis applications. Nonetheless, due to its flexibility and 'green' character, this technology is still commonly utilized.[32]

The main material, referred to as saccharide carbon dot, was synthesized using hydrothermal treatment employing D-glucose, D-galactose, and D-lactose as carbon sources. Dr. Roger M. Leblanc, a renowned researcher associated with the Department of Chemistry at the University of Miami in Florida, developed the saccharide carbon dots used in this study. The process of preparing the CDs starts by inserting a volume of 20 mL of a saccharide solution with a concentration of 0.3 M into a reactor coated with Teflon. This reactor is then positioned within a muffle furnace. After being heated to 200 °C for 30 minutes, the reactor underwent a subsequent 5-hour period during which the temperature remained constant at 200 °C. After subjecting the mixture to centrifugation at a speed of 9000 revolutions per minute for a duration of 20 minutes, a substantial, dark-colored solid mass was obtained. The remaining liquid portion, known as the supernatant, was subsequently passed through a filter with a pore size of 0.2 micrometers to eliminate any insoluble particles. The pH of the solution was manipulated and subjected to dialysis for a duration of three days using deionized water. The dialysis procedure was conducted employing a dialysis membrane with a molecular weight cut-off (MWCO) of 1 kDa. Subsequently, the resulting sample was subjected to lyophilization, resulting in the formation of a solid product.[11]

Neuroblastoma

Neuroblastoma is the prevailing non-brain solid tumor in children below the age of five. After road accidents, neuroblastoma is the leading cause of fatalities among society's youngest members. Neuroblastoma has a fatality rate of at least 15%.[33] Dopamine, a type of catecholamine metabolite, is utilized as a diagnostic tool in the identification of neuroblastoma. It is also employed in clinical diagnosis and early detection through screening programs.[34] A urinalysis (urine test) may also be done to help check kidney function and detect urinary dopamine levels.

Detecting biomarkers for cancer in earlier stages increases the potential for a positive prognosis. Therefore, the aim of this research is to develop an easily utilized test and analytical technique to detect one of the common biomarkers for neuroblastoma: dopamine.

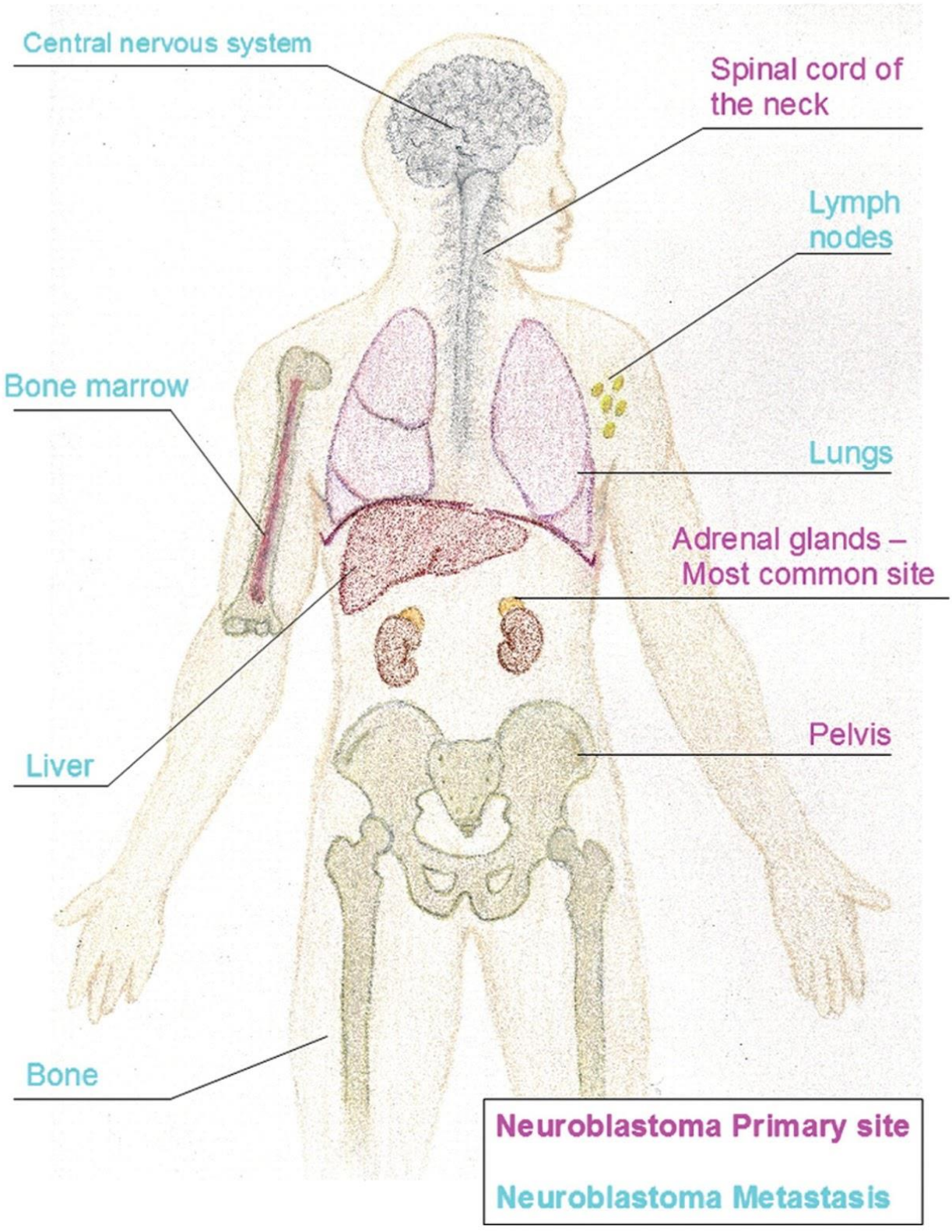

Fig 3: Diagram showing neuroblastoma and primary site of location.[35]

Dopamine

Dopamine, scientifically referred to as 4-(2-aminoethyl) benzene-1,2-diol (DA), is a type of neurotransmitter that is synthesized by neurons in the brain. It serves a crucial role in transmitting neurological signals.[36] Dopamine exerts a substantial influence on various physiological systems in the human body, including the metabolism, central neurological system, renal system, and hormonal system. Insufficient levels of dopamine can lead to many neurological disorders, such as Parkinson's disease and schizophrenia.[37] Dopamine levels in different human biofluids exhibit physiological variations. As per the Human Metabolome Database, the blood content of Dopamine is below 130 picomolar (pM), however it is 5 nanomolar (nM) in human cerebrospinal fluid and urine.

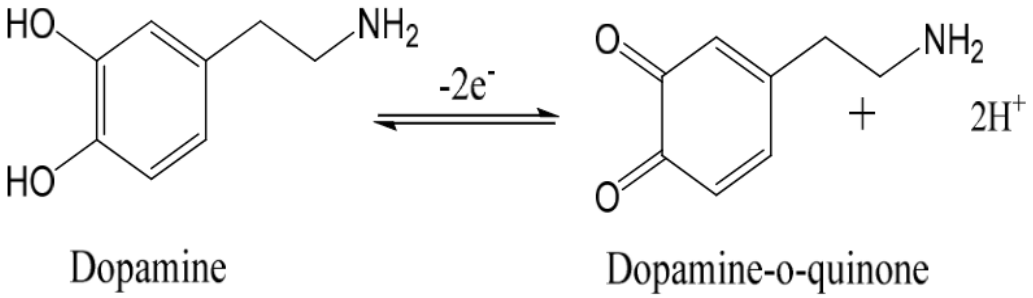

Figure 4: Dopamine / Dopamine-o-quinone redox [38]

As a result, the detection and quantification of dopamine in vivo and in vitro are important topics in medical practice. For the dopamine assay, several techniques have been used, including electrochemical analysis, liquid chromatography, and spectroscopic fluorescence. Electrochemical analysis has garnered significant interest due to its exceptional sensitivity, rapid response, affordability, and user-friendly nature.[39]

ELECTROCHEMICAL TECHNIQUES AND ANALYSIS

Electrochemical method

Electrochemical techniques are extensively utilized in various applications due to their exceptional selectivity, accuracy, and precision. Voltammetry is the primary electrochemical technique employed to quantify the resultant electric current.

Cyclic Voltammetry

Cyclic voltammetry (CV) is a very efficient and adaptable electroanalytical technique that is often used for preliminary electrochemical investigations. CV was employed in the domains of electrochemistry, inorganic chemistry, organic chemistry, and biochemistry due to its convenience in measurement.[40] Cyclic voltammetry (CV) is a technique employed to investigate electrochemical processes occurring on an electrode surface. It is known for its ability to rapidly provide valuable insights into the thermodynamics of redox reactions.[41] The voltammogram in the cyclic voltammetry experiment is acquired using a potentiostat. A voltammogram is a graphical representation of the relationship between the electric current (I) and the electric potential (E). The present measured value is a consequence of the redox reaction of the analyte, which is characteristic of electrochemical reactions. A voltammogram exhibits a curve that signifies a redox cycle. The voltammogram displays a current scale on the y-axis, ranging from -y to +y. The positive values correspond to oxidation, while the negative values correspond to reduction. Three different electrodes and an electrochemical cell were used in the cyclic voltammetry studies. A platinum wire counter electrode was employed to commence the current flow at the onset of the analyte's redox reaction. The Ag/AgCl reference electrode, with a concentration of 3.5 M AgCl,

served as a benchmark to evaluate the potential of other electrodes. The working electrode is a freshly produced Nafion/Saccharide/GCE. When the analyte undergoes a redox reaction, this working electrode serves as a conduit for the flow of electrons.

Chronoamperometry

Chronoamperometry is a method in which a constant voltage is provided to the working electrode (compared to the reference electrode) and the current flowing through the electrode is measured over a period of time. The current-time response consists of two distinct components: the current resulting from the charging of the double layer and the current arising from the electron transfer mechanism involving the electroactive species.[42] High charging currents are generated by chronoamperometry, but they diminish exponentially with time, just like any RC circuit would. Compared to other amperometry techniques, the enhanced signal-to-noise ratio of CA is a consequence of integrating the current over a longer time interval.43 This method can also be employed to quantify the spread of an electroactive substance. When the working electrode takes the form of a flat electrode, the diffusion coefficient can be determined by analyzing the inclination of the linear regression line obtained from a plot of current versus time, commonly referred to as a Cottrell plot. The Cottrell equation provides the mathematical expression for this linear diffusion.

$$I(t) = \frac{nFAD^{1/2}C}{t^{-1/2}} = kt^{-1/2}$$

Analytical Techniques

Nanomaterial characterization has emerged as a crucial component of nanotechnology throughout the past decade. Diverse methodologies have been employed to analyze and investigate these nanomaterials, including Raman spectroscopy and scanning electron microscopy (SEM). The identification of the dopamine nanocomposite synthesized in this investigation was conducted utilizing these analytical methodologies.

Raman spectroscopy

Raman spectroscopy is a quick, non-destructive, and high-resolution method for characterizing the lattice structure and the electronic, optical, and phonon characteristics of carbon materials, such as three-dimensional diamond and graphite, two-dimensional graphene, one-dimensional carbon nanotubes, and carbon dots.[44]

Raman spectroscopy is employed to analyze the diamond bands of carbon dots, and the ratio of the intensity between the D and G bands in Raman scattering is frequently utilized to evaluate the level of defects in carbon materials. The carbon dots with larger ratios of sp^2-sp^3 hybridized carbon have a positive correlation with increased electrochemical sensitivity, as determined by the measured Raman (I_G/I_D) intensities. [45]

Peaks in the Raman spectrum represent the wavelength and intensity position of the Raman scatter light. Each peak corresponds to a distinct vibration of a chemical bond, including single bonds such as C-C, C=C, N-O, and C-H, as well as groups of bonds such as benzene ring, lattice chain, and polymer chain vibrations.[46] The D band is known as the disordered band because it is related

with the vibrational state of an sp^3 hybridized carbon atom, whereas the G band is known as the graphitic band because it is associated with the vibrational state of a sp^2 hybridized carbon atom.[47]

Scanning electron microscopy

Several microscopy techniques have been introduced in recent decades to investigate the attachment and structure of cells on different biomaterials. Scanning electron microscopy (SEM) is widely acknowledged as the most feasible choice for visualizing and analyzing the three-dimensional architecture of objects in the realm of electron microscopy technologies.[48] It is indisputable that scanning electron microscopy possesses an unparalleled spectrum of capabilities, making it unrivaled by any other instrument. The organic chemicals are polymerized to make bigger molecules, which is what happens in the hydrothermal reactor to make the carbon quantum dots.[49]

Scanning electron microscopy is commonly employed to examine large samples with a resolution of around 1 nm, encompassing the micrometer dimensions of whole cells to labeled molecules. The device operates by employing an accelerated electron beam with a wavelength that is 100,000 times smaller than that of light photons. This enhances the magnification capability of light microscopes (200 nm) by a factor of 1000 (0.2 nm).[50]

A focused ion beam column, also known as a FIB column, is a feature that can be found in many types of SEM. This feature makes it possible to extract electron-transparent samples from precise regions inside bulk materials.

Fig 5: Image showing Hitachi S-3400 N scanning electron microscope

When used in conjunction with a FIB and a transmission detector, the SEM and its numerous detectors provide a sophisticated combination of tools for sample preparation, imaging, diffraction, and analysis, with practical length scales ranging from nanometers to several centimeters.[51]

CHAPTER II

EXPERIMENTAL METHODOLOGY

In this research, Carbon dots were synthesized or developed to detect dopamine by various electrochemical techniques and analytical techniques such as cyclic voltammetry, chronoamperometry, scanning electron microscopy, etc. The glassy carbon electrode used in my research has a dimension of 5mm, and the saccharides (D-lactose, D-glucose, and D-galactose) were used as carbon sources, which were provided to us by the chemistry department at the University of Miami.

Different instruments used for analysis

Instruments used in this research for different analysis purposes:

a. Digital analytical balance (Mettler AE-163, New Jersey, USA)

b. Ultrasonic cleaner (Sharpertek Stamina XPTM, WI, USA)

c. Water de-ionizer (ELGA, High Wycombe, UK)

d. pH meter (Thermo electron corporation, Orion 230 A+, MA, USA)

e. Oven (Thelco Laboratory, CA, USA)

f. Magnetic Stirrer (Fisher Scientific, MA, USA)

g. WaveNano USB potentiostat (Pine instrument, Raleigh, NC, USA)

h. Scanning Electron Microscopy, SEM (Hitachi H-7650, Krefeld, Germany)

i. Raman Spectroscopy (Enwave Optronics, Inc., Model-uSense-I-785, Irvine, CA, USA)

Chemicals and Materials

a. Glassy Carbon Electrode (Pine Instruments, Raleigh, North Carolina, USA)

b. Dopamine (Sigma-Aldrich, St. Louis, MO, USA)

c. Glucose (Sigma-Aldrich, St. Louis, MO, USA)

d. Uric acid (Sigma-Aldrich, St. Louis, MO, USA)

e. Nafion (Ion Power, Inc, New Castle, Delaware, USA)

f. Absolute anhydrous isopropyl alcohol (AAEA) (Pharmaco-AAPER, Brookfield, CT)

g. Nafion (Ion Power, New Castle, Delaware, USA)

h. 1:1 mixture of HNO_3:H_2O (Fisher Scientific, Pittsburg, USA)

i. MicropolishTM Alumina, 0.05μm (Lake Bluff, IL, USA)

j. Micropolish™ Alumina, 1.00μm (Lake Bluff, IL, USA)

k. Phosphate Buffer Solution (PBS), pH 7.00 (Sigma-Aldrich, St. Louis, MO, USA)

l. Saccharide Carbon Dots (D-lactose, D-sucrose, and D-galactose):

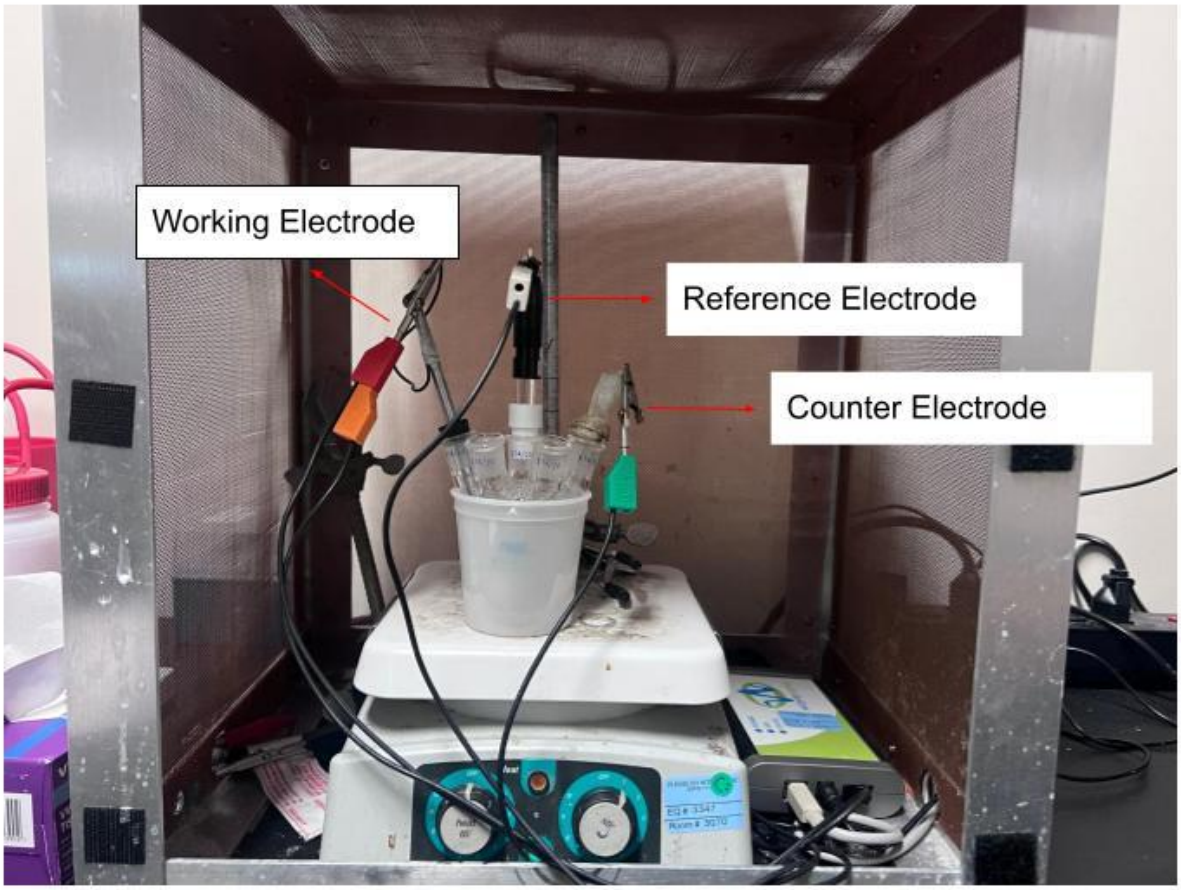

Fig 6: An instrumental setup inside the Faraday cage for CV experiments.

The electrochemical cell used during cyclic voltammetry experiments

a. Working electrode, D-lactose-CDs/GCE

b. Counter electrode, a Platinum wire,

c. Reference electrode, Ag/AgCl (3.5 M KCl)

Synthesis and Preparation of saccharide carbon dots

The principal material, known as saccharide carbon dot, was produced through hydrothermal treatment utilizing D-glucose, D-galactose, and D-lactose as carbon sources. Dr. Roger M. Leblanc, a distinguished researcher affiliated with the Department of Chemistry at the University of Miami in Florida, created the saccharide carbon dots utilized in this study. The preparation of the CDs commences with the introduction of a 20 mL volume of a saccharide solution, having a concentration of 0.3 M, into a Teflon-coated reactor. Subsequently, the reactor is placed within a muffle furnace. Following a 30-minute heating process at 200 °C, the reactor experienced a further 5-hour period with a constant temperature of 200 °C. Following centrifugation of the mixture at a rate of 9000 revolutions per minute for a period of 20 minutes, a significant, dark-colored solid mass was acquired. The residual liquid component, referred to as the supernatant, was then filtered using a 0.2 millimeter pore size filter to remove any insoluble particles. The solution's pH was adjusted and then dialyzed for a period of three days using deionized water. The dialysis technique was performed using a dialysis membrane with a molecular weight cut-off (MWCO) of 1 kDa. Afterwards, the obtained sample underwent lyophilization, leading to the production of a solid product.[52]

Attaching the Saccharide carbon dots (D-lactose, D-glucose, and D-galactose) with a glassy carbon electrode for electrochemical sensing

A suspension of saccharide carbon dots was generated by combining 0.5 mg of CDs with 1 mL of absolute anhydrous ethanol (Pharmaco-AAPER, Brookfield, CT, USA) in an Eppendorf tube. The colloidal CD suspensions were prepared by subjecting them to sonication for a duration of 5 minutes. The saccharide carbon dots were employed for the modification of the working electrode of the GCE. Prior to alteration, the surface of the glassy carbon electrode (GCE) was polished using alumina slurries with diameters of 1.0 μm and 0.05 μm for approximately 3-5 minutes in succession. Subsequently, the GCE surface had a thorough rinsing with ultrapure water and was subjected to 5 minutes of sonication during each polishing phase. In addition, the electrode surface was subjected to sonication using a concentrated mixture of HNO_3:H_2O for a duration of 5 minutes in order to activate the surface. Subsequently, the GCE surface was desiccated with Kim wipes at ambient temperature. A 10-μL portion of the saccharide CDs suspension was placed on the 5mm-diameter electrode that had just been polished, and then left to dry at room temperature. An additional 10-microliter droplet of Nafion, a binder with a weight percentage of 2%, was added to the modified GCE surface to cover and secure the CDs onto the electrode surface. The altered GCE was subsequently dehydrated in an oven for a duration of 30 to 40 minutes at a temperature of 40 °C. Ultimately, the GCE electrode was adapted to specifically detect dopamine.

Electrochemical study of Dopamine using the Polished modified Saccharide GCE

An experiment was carried out to examine the electrochemical properties of dopamine utilizing a refined and altered saccharide glassy carbon electrode (GCE). The effort involved the utilization of cyclic voltammetry (CV) and chronoamperometry techniques. The experiment took place inside

a custom-built Faraday cage made of a copper grid with a mesh size of 10 and a diameter of 0.025 inches. The cage was designed with the intention of minimizing external interference, namely disruptions occurring at a frequency of 60 Hz.. The Wavenano potentiostat electrochemical software, developed by Pine Instruments Company in Raleigh, NC, USA, was utilized for data acquisition and analysis. The experimental setup included a 3-electrode cell configuration for the measurements. The setup consisted of a reference electrode consisting of Ag/AgCl (3.5 M KCl), a counter electrode constructed of platinum wire, and a glucose-modified glassy carbon electrode (GCE). The measurements were conducted in a controlled environment of an inert N2 atmosphere at ambient temperature, namely 22 °C. The entire setup was contained within a custom-built Faraday cage. The potential range was established as -0.10 to +0.10 V, with a scan rate of 50 mV/s. The peak potential corresponding to a certain analyte was chosen from the results obtained in the cyclic voltammetry experiment. The concentration of the analyte, dopamine HCl, spans from 0.01 mM to 0.1 mM and from 0.1 mM to 1 mM.

Additionally, a comparative analysis was conducted on the cyclic voltammetry of two distinct analytes: D-glucose and uric acid, both at a concentration of 1 mM. The resulting peak heights of these concentrations were then compared to those of dopamine HCl, both at a concentration of 1 mM.

CHAPTER III

RESULTS AND DISCUSSION

Chronoamperometry

Based on the results of the electroanalysis 2021 paper, a chronoamperometry experiment was attempted for dopamine detection at concentrations ranging from 0.01mM to 1mM. The waveNano potentiostat was adjusted to a potential of +0.5824 V in order to conduct chronoamperometric measurements of the oxidation peak. However, this did not work as the lactose glassy carbon electrode composite did not show a good signal at the potential of +0.5824 with a scan rate of 50 $m.Vs^{-1}$.

Cyclic Voltammetry

The cyclic voltammetry technique was used to study the electrocatalytic behavior of the Nafion/Saccharide GCE composite towards dopamine (DA). This explains the redox reaction that occurs between the dopamine and the surface of the working electrode, a 5 mm diam glassy carbon electrode doped with a suspension of the carbon dots and 2wt% Nafion was used. Below are the CVs of the three composites of saccharide carbon dots (glucose, galactose, lactose) in a 1 mm concentration of Dopamine solution at pH 7.0.

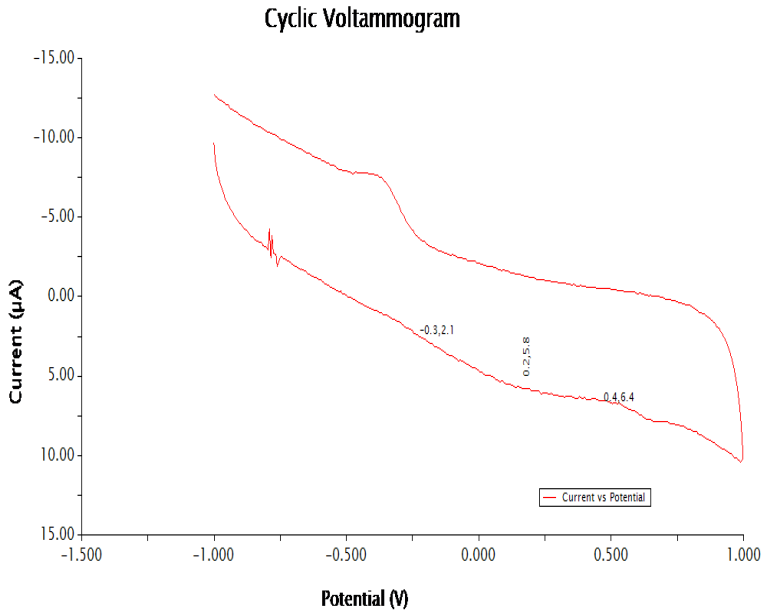

Fig 7: A cyclic voltammogram PBS (blank)

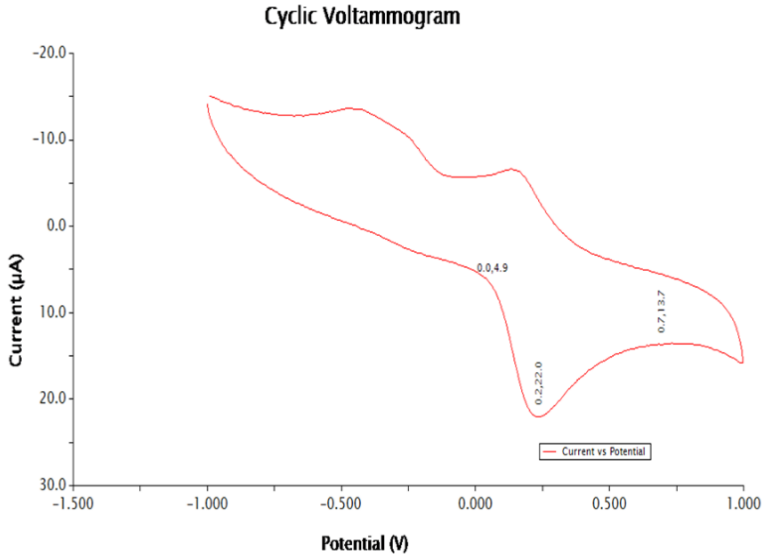

Fig 8: A cyclic voltammogram of 1mM dopamine using Galactose carbon dots

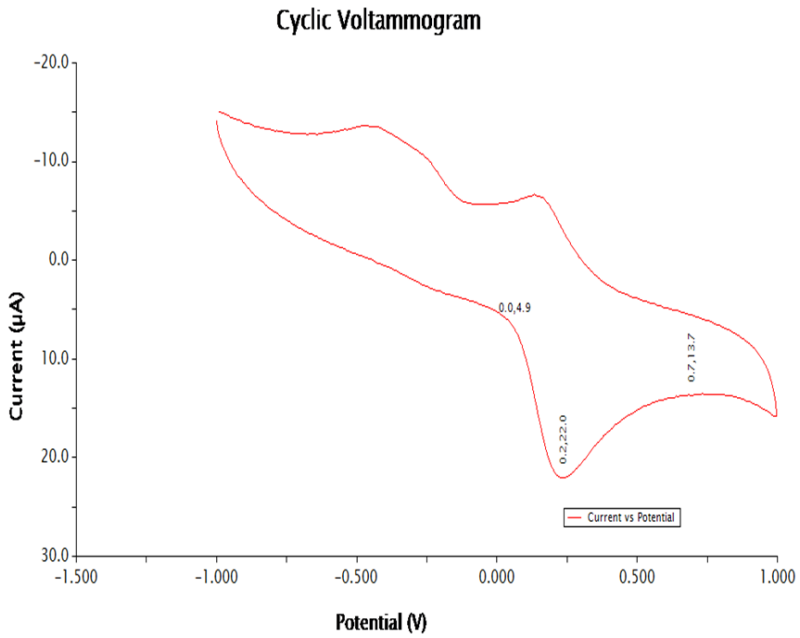

Fig 9: A cyclic voltammogram of 1mM dopamine using Glucose carbon dots.

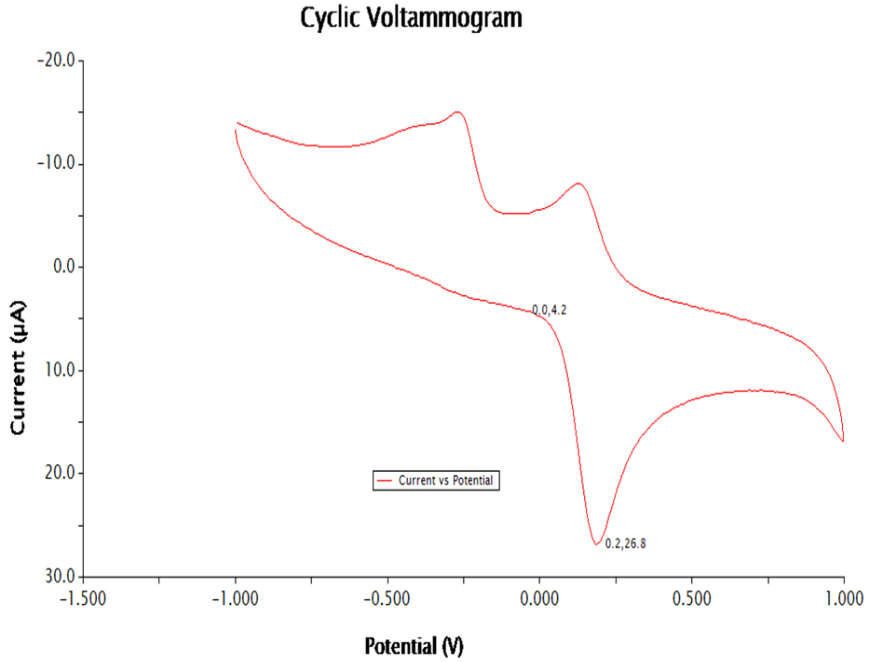

Fig 10: A cyclic voltammogram of 1mM dopamine using Lactose carbon dots

The figures above show CVs at 50 mVs^{-1} of 1mM DA.Hcl in PBS =7.0 using carbon dots prepared from Galactose, Lactose, and Glucose. The CV line shape indicates a quarsireversible redox taking place with two reduction peaks and one oxidation peak for all of the three carbon dots used. For the saccharide carbon dots, the Lactose CDs have the highest intensity followed by Glucose CDs and then Galactose CDs with maximum oxidation peaks set to be 23.0, 17.4, and 6.2 μA respectively.

CV current measurement for 1mM Dopamine HCl

CARBON DOTS	Lactose	Galactose	Glucose
CURRENT	23.2	6.20	17.7
	23.2	6.20	18.2
	22.6	6.20	17.4
MEAN	23.0	6.20	17.8
STANDARD DEVIATION	0.35	0	0.400

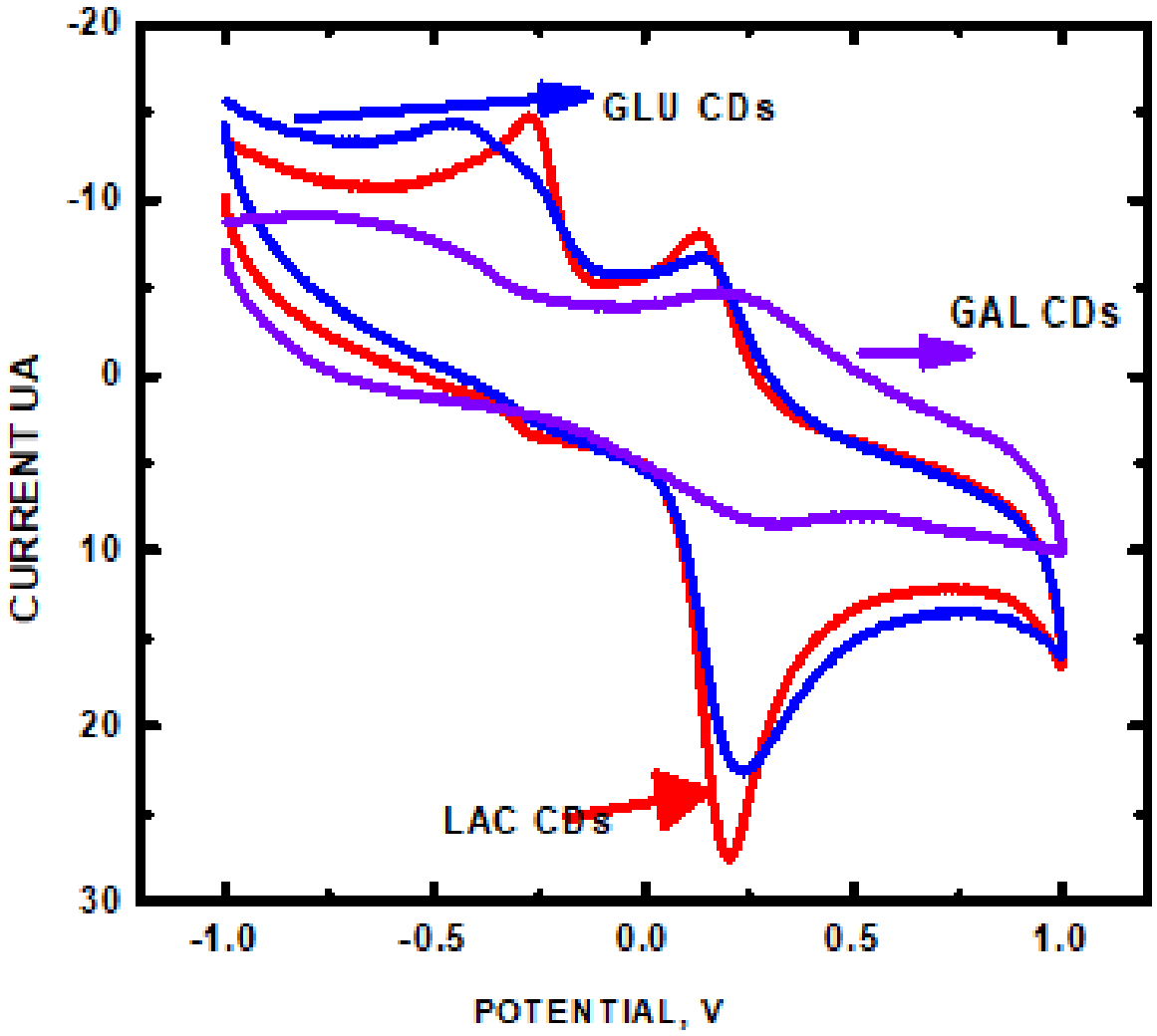

Fig 10: Stack plot for the Gal, Glu, and Lac CDs [1mM Dopamine, PBS (pH 7)]

This shows the stack plot for the three saccharide carbon dots. From the plot, Lactose CDs has the highest sensitivity to 1mM dopamine. This comes from measuring the peak current from baseline. The oxidation peaks were the most pronounced for the lactose carbon dots composite applied to the working electrode, with loading for all three carbon dots identified.

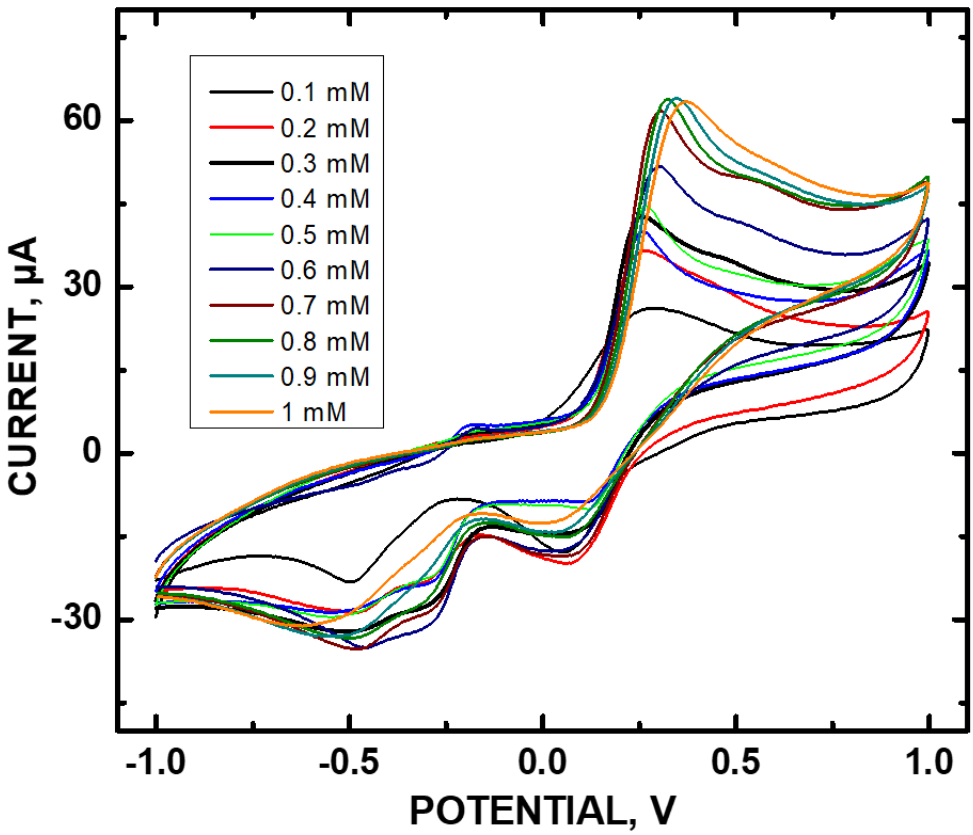

Fig 11: Stack plot of 0.1mM – 1.0mM of Dopamine using Galactose CDs

The stack plot above shows the Cyclic voltammetry response of Galactose CDs under different concentrations of dopamine hydrochloride from 0.1mM - 1.0mM. From the plot, 1.0mM elicit the highest current sensitivity. Also, these CVs indicate the increase in peak current as the concentration of DA increases from 0.1mM to 1.0Mm

3.3 Electrocatalytic Study of various CVs of Lactose CDs ranging from 0.01µm - 0.1µm and 0.1µm - 1µm 0f DA-HCl

The Nafion/Saccharide GCE composite was used as the working electrode to carry out all the CV experiments for various concentration of dopamine under pH 7.0. The two figures below show the overlay of two concentration ranges from the cyclic voltammogram. These CVs show that the concentration is directly proportional to the peak current. As the concentration increases from 0.01µm - 0.1µm and 0.1µm - 1µm the peak current also increases with 1µm having the highest peak current.

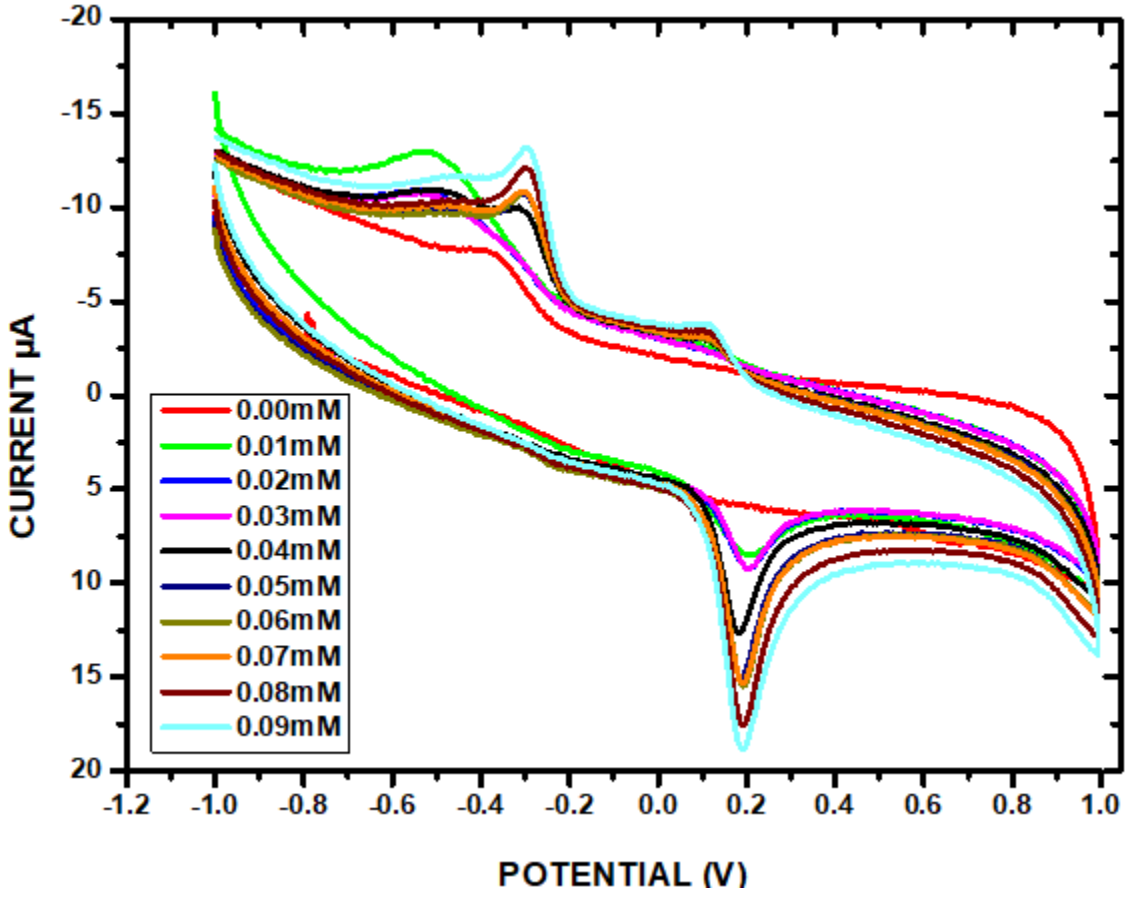

Fig

Fig 12: Stack plot of cyclic voltammogram of 0.01mM - 0.1mM Dopamine HCl on Lactose CDs

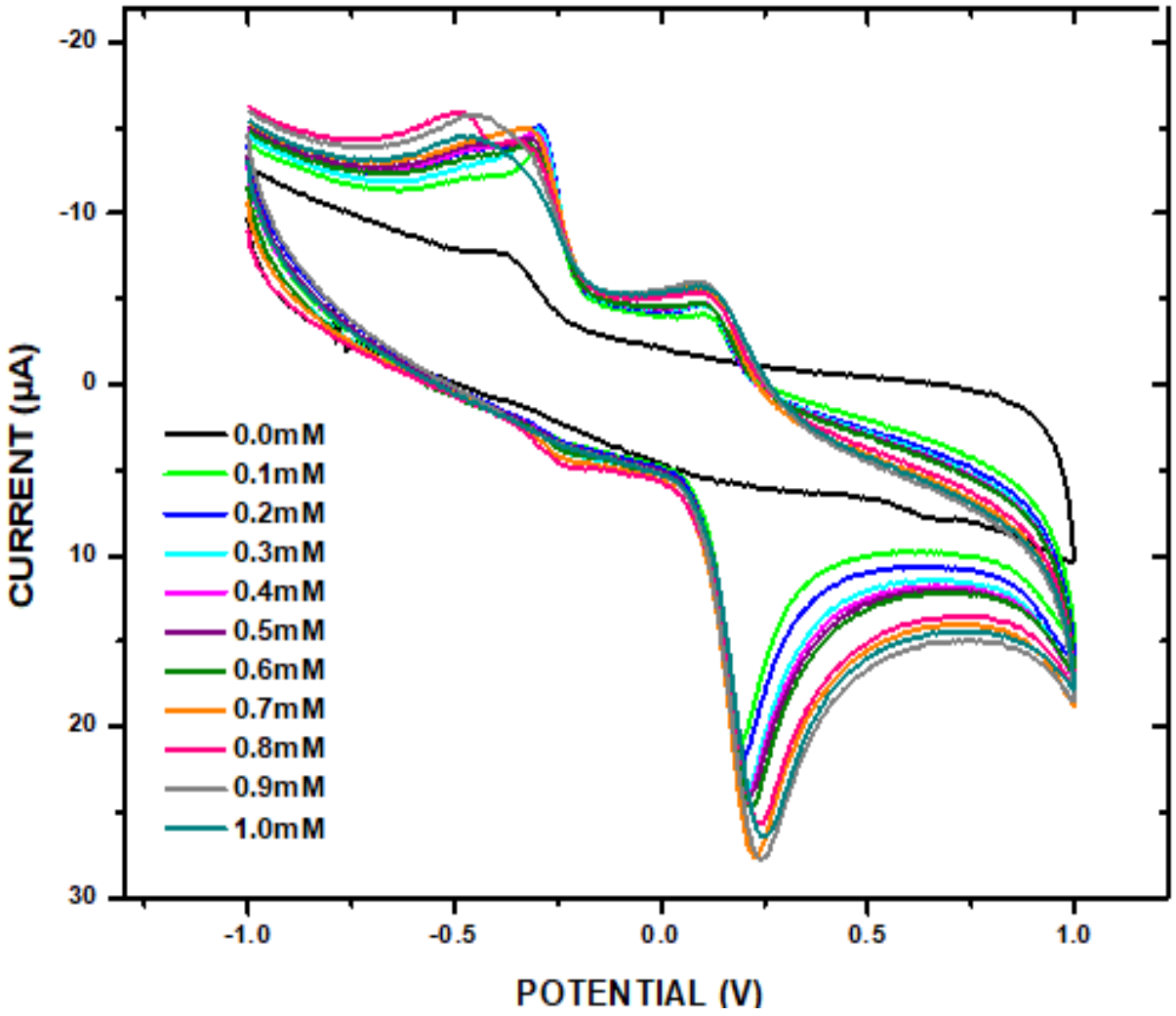

Fig 13: Stack plot of cyclic voltammogram of 0.1mM - 1mM Dopamine HCl on Lactose CDs

3.4 Linear calibration plot for the Saccharide carbon dots

The figure below displays the linear calibration curve for galactose carbon dots at concentrations ranging from 0.1 mM to 1 mM. This illustrates the efficacy of cyclic voltammetry in detecting a wide range of concentrations, including galactose, which has the lowest sensitivity. The paper 'Graphene defects in saccharide carbon dots govern by electrochemical sensitivity' assessed the electrochemical sensing properties of Galactose, Lactose, and Glucose carbon dots. The results indicate that the Galactose carbon dots exhibit the most prominent CV peaks, indicating the highest sensitivity for detecting acetaminophen. This provides us with a justification to construct a calibration plot for different concentrations of GalCDs to detect dopamine.

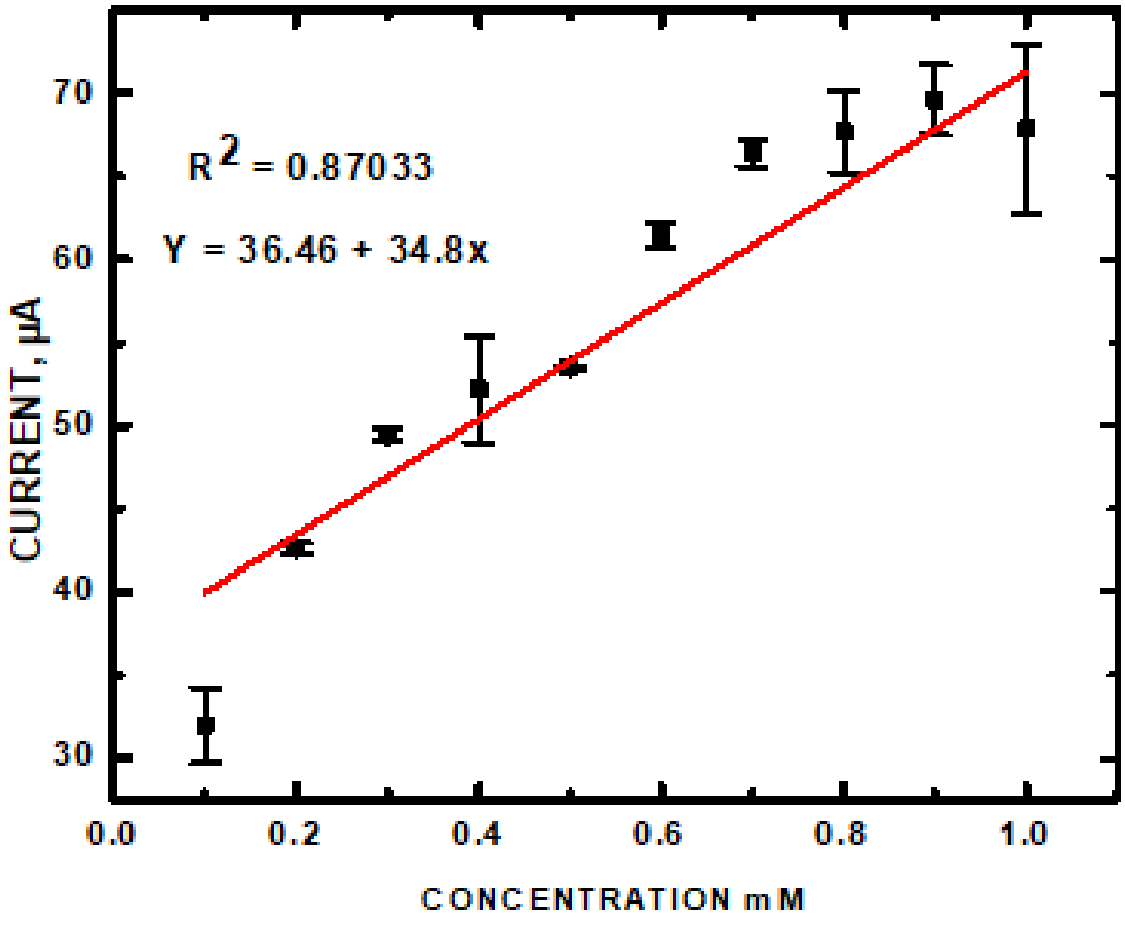

Fig 14: Linear Calibration plot for 0.1mM – 1mM DA with Galactose carbon dot

The table below shows the concentration from 0.01mM – 0.1mM of dopamine HCl and the average current for Lactose CDs.

Concentration (mM)	Current 1 (µA)	Current 2 (µA)	Current 2 (µA)	Average current (µA)	S.D
0.01	4.10	3.90	4.10	4.03	0.120
0.02	4.00	4.30	4.20	4.17	0.150
0.03	4.30	4.80	6.00	5.03	0.870
0.04	7.90	9.70	8.90	8.83	0.900
0.05	9.80	9.30	9.90	9.67	0.320
0.06	10.2	10.1	9.80	10.0	0.210
0.07	10.1	10.6	11.2	10.6	0.550
0.08	11.5	12.0	12.9	12.1	0.710
0.09	13.8	14.3	15.3	14.5	0.760
0.1	15.8	15.7	14.6	15.4	0.670

The table below shows concentration from 0.1mM – 1mM of dopamine and the average current

Concentration (mM)	Current 1 (µA)	Current 2 (µA)	Current 3 (µA)	Average current (µA)	S.D
0.1	15.8	15.7	14.6	15.4	0.670
0.2	16.3	17.9	18.3	17.5	1.06
0.3	18.4	18.3	19.1	18.6	0.440
0.4	18.9	18.9	18.6	18.8	0.170
0.5	19.1	18.9	19.1	19.0	0.120
0.6	19.4	19.4	19.4	19.4	0.000
0.7	20.4	20.3	21.3	20.7	0.550
0.8	21.0	20.9	20.9	20.9	0.0600
0.9	22.1	21.7	21.0	21.6	0.57
1.0	22.3	21.1	23.0	22.1	0.96

The linear calibration plot and table for 0.01mM – 0.1mM Dopamine HCl with Lactose carbon dots

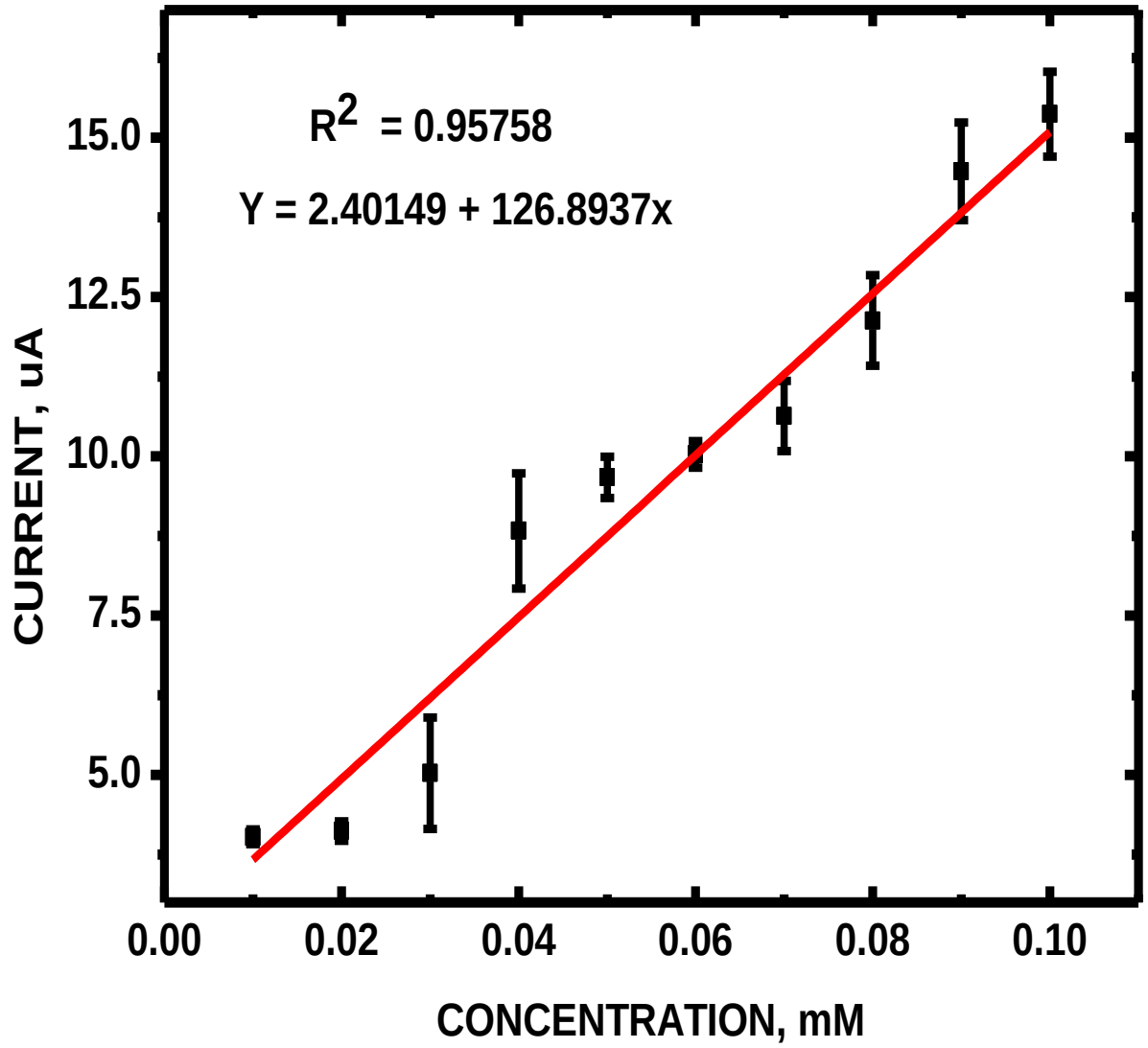

Fig 15: Current versus concentration plot of 0.01mM - 0.1mM Dopamine HCl with Lactose CDs

Fig 15 shows the current vs concentration plot. there is a linear relationship from 0.01 mM to 0.1mM dopamine concentration. Here, the I_{pc} =127 [dopamine] + 2.40 with correlation coefficient (R^2) of 0.957

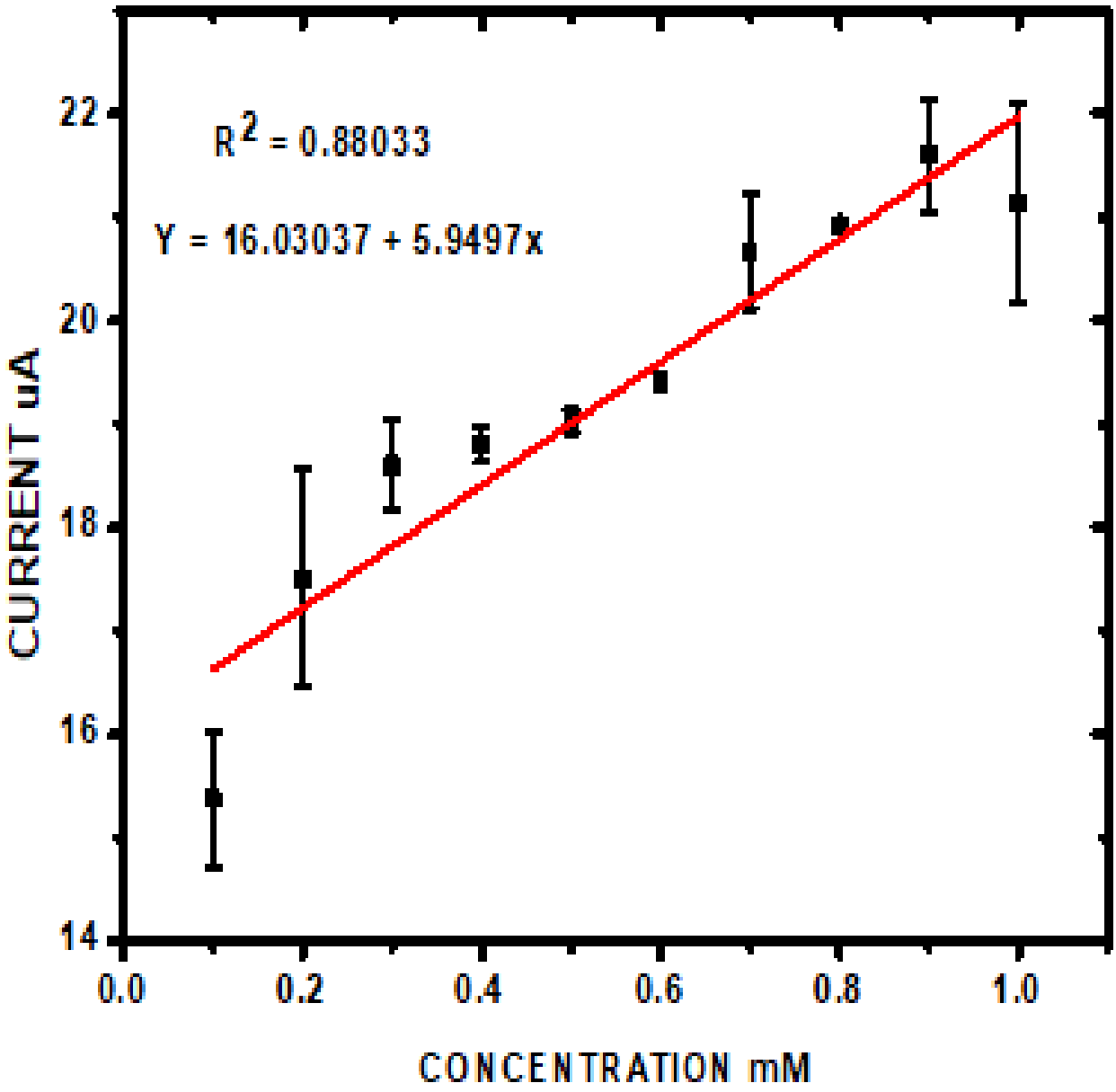

Fig 16: Current versus concentration plot of 0.1mM - 1mM Dopamine HCl with Lactose CDs

Fig 16 shows the current vs. concentration plot. There is a linear relationship from 0.01 mM to 0.1 mM dopamine concentration. Here, the Ipc = 5.95 [dopamine] + 16.0, with a correlation coefficient (R^2) of 0.880.

The concentration ranges of (0.01mM - 0.1mM) and (0.1mM - 1mM) exhibit distinct slopes of 127 and 5.95, respectively, due to the increasing saturation of the surface sites of lactose carbon dots on the glassy carbon electrode at higher concentrations.

As we combined the linear plots of 0.01 mM - 0.1 mM and 0.1 mM - 1 mM of dopamine HCl, a fifth-degree polynomial curve was obtained.

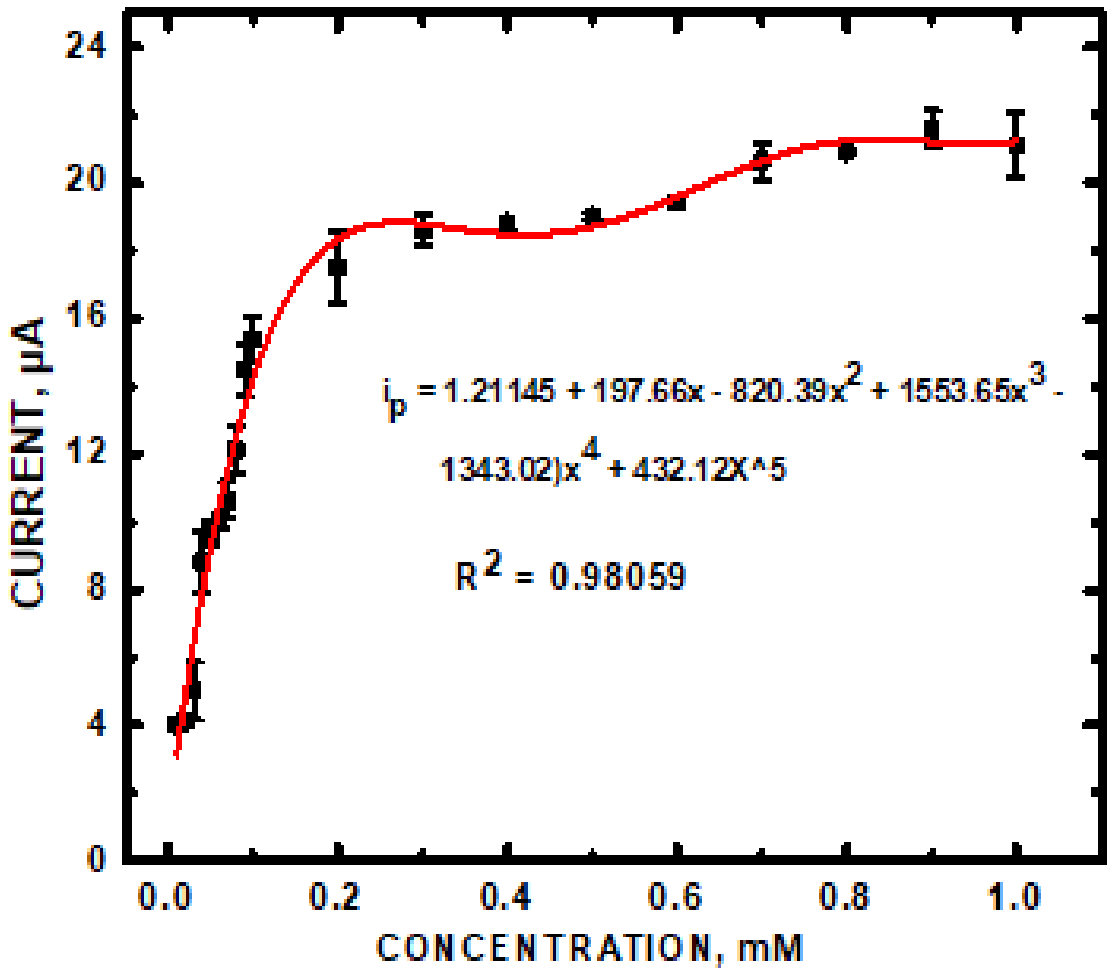

Fig. 17: Calibration curve in response to current and increasing concentration of dopamine HCl from (0.01-1) mM.

The least squares fitting of the plot was performed using Origin Pro B.S. This is a plot showing the analytical range from 0.01 mM to 0.1 mM. This follows a fifth-order polynomial equation, which is a functional calibration plot. The plot demonstrates that the line becomes increasingly steep when the concentration reaches 0.1mM. This phenomenon can be explained by the presence of impurities on the surface of the glassy carbon electrode that accumulate over time during continuous usage.

Dopamine detection limit

Dopamine detection limit is the smallest quantity of dopamine concentration that is significantly different from the blank.

Signal detection limit = y_{blank} + 3s

y_{blank} = 7.9 µA

Standard deviation = 0.35 µA

Signal detection limit = 7.9 µA + 3 (0.35 µA) = 8.95 9 µA

The minimum detectable concentration = $\frac{3s}{m}$

m = slope, s = standard deviation

The minimum detectable concentration = $\frac{3\ (0.35\ \mu A)}{127} = 0.008$ mM

The minimum detectable concentration for dopamine with lactose carbon dots is 0.008 mM.

Selectivity study of Lactose carbon dot towards Dopamine, D-glucose, and Uric Acid

Dopamine, which is a catecholamine present in urine, provides the mainstay for biochemical testing of neuroblastoma. Urinary excretion contains several biological compounds in certain concentrations that may interfere with the neuroblastoma screening process, with Uric acid and D-glucose serving as the major interfering analytes. These two analytes were used in a selectivity study of lactose carbon dots towards dopamine HCl. Fig. below shows that the response of lactose CDs to GCE was quite selective for dopamine HCl at the oxidation potential, with little or no current response towards the other two analytes (uric acid and D-glucose).

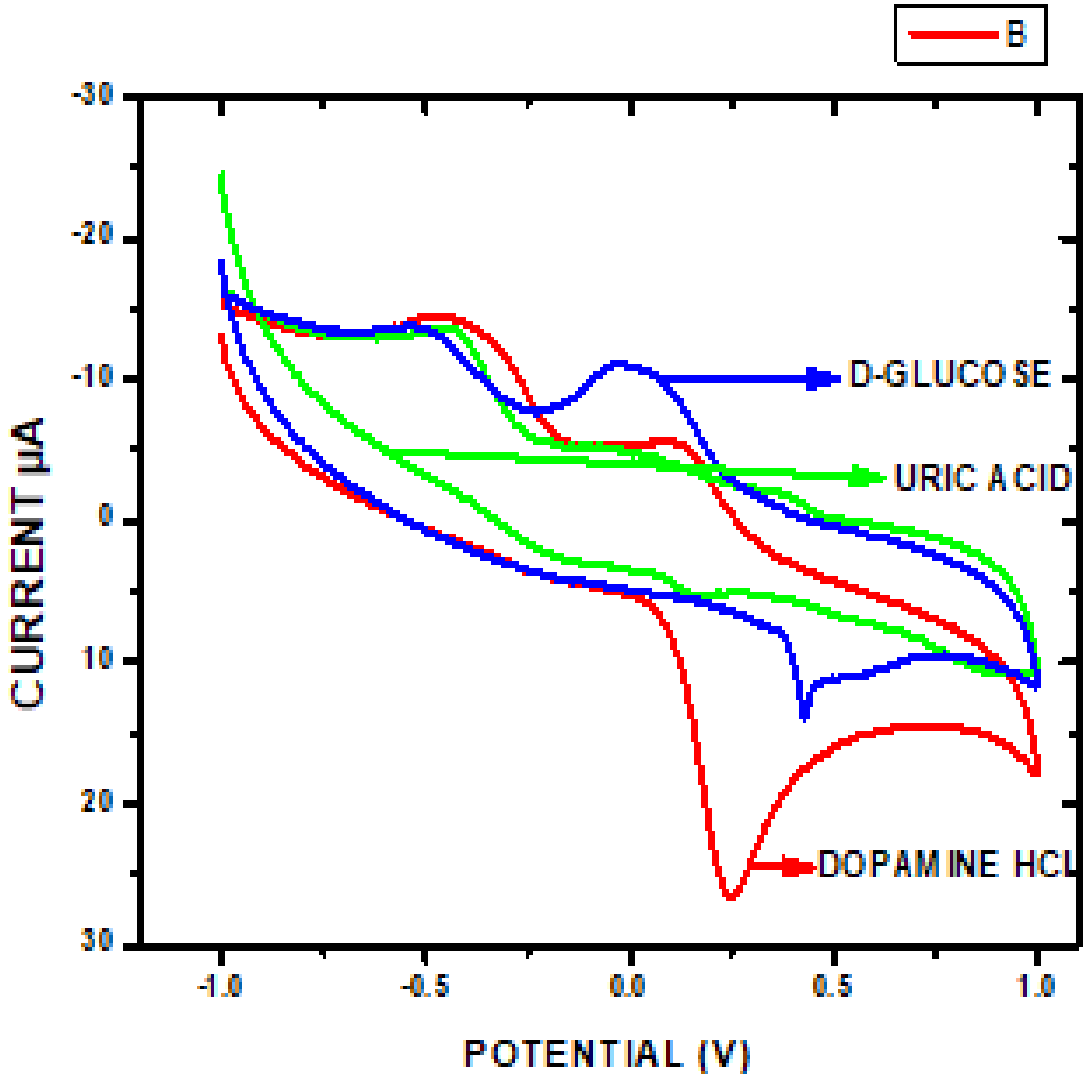

Fig 18: Cyclic Voltammogram response of 1mm concentration of Dopamine, Uric acid, and D-glucose towards Lac CDs

Scanning Electron Microscope (SEM)

In scanning electron microscopy (SEM), the lactose CDs sample is subjected to a high-energy electron beam. This causes the accumulation of charge, resulting in a picture that provides information about the shape, surface features, and arrangement of the granules. The scanning electron microscope (SEM) image in figure 19 reveals that the nanomaterials and composite consist of lactose carbon dots, which predominantly exhibit a spherical morphology and possess particle sizes that are randomly distributed. The particles exhibited a dense arrangement, with only a limited number of sparsely distributed particles. The density of these particles can be verified by certain sections of the micrograph following exposure to sonication and application over the glassy carbon electrode using a 10µl volume. Figure 19 displays the scanning electron microscope (SEM) image of the glassy carbon electrode (GCE), while Figure 20 presents the histogram illustrating the distribution of sizes. The ImageJ software was utilized to quantify the diameter of the nanoparticles, which were subsequently employed to construct a size histogram. The histogram displays the mean diameter of 156 (±7) nm. The carbon dots exhibited a rather consistent average size, with little variations in diameter. Their consistent similarity enables the highest level of dopamine oxidation peak current as a result of their rapid electron transfer capabilities and larger surface area.

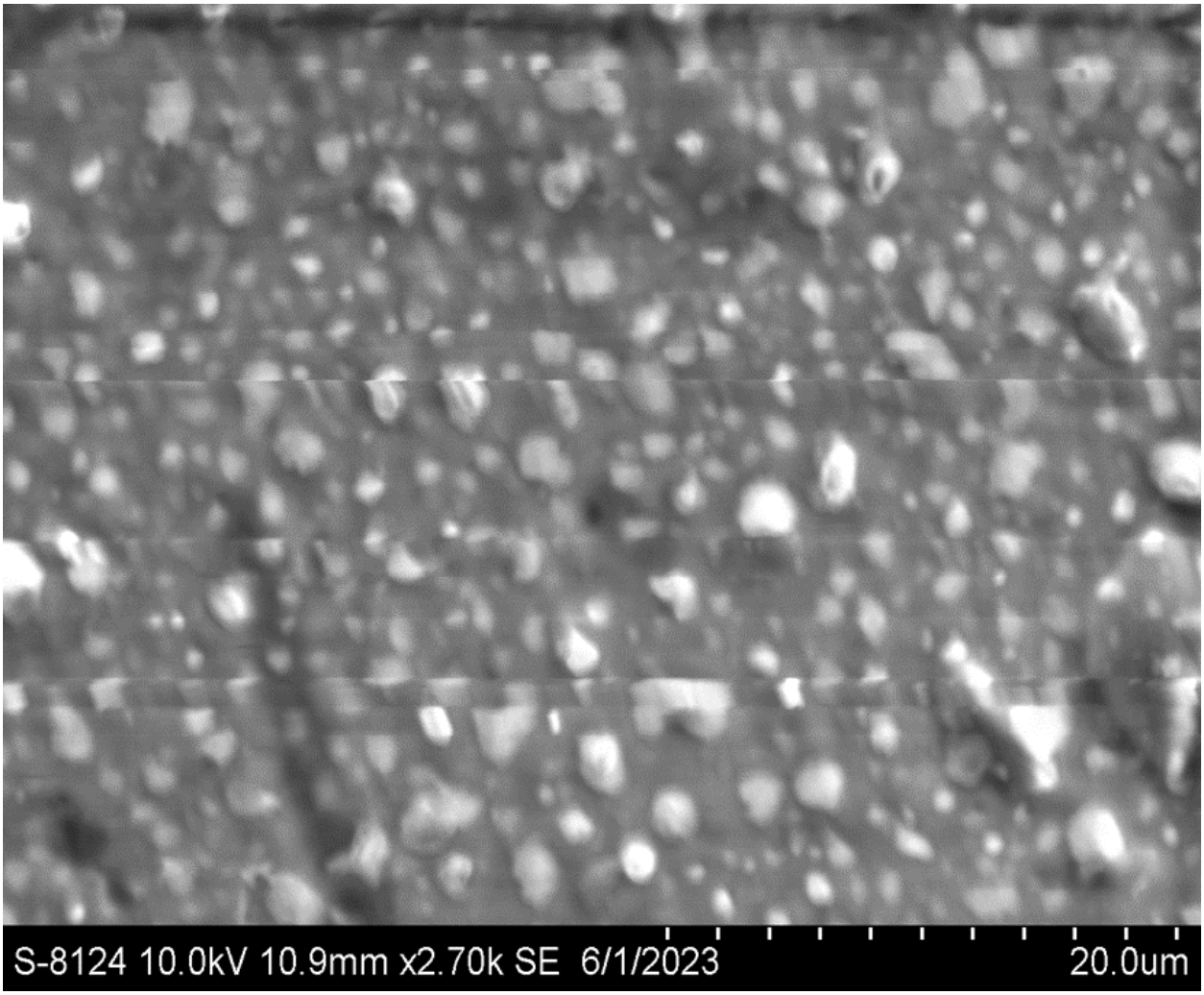

Fig 19: SEM image of optimized GCE with 10 µl Lac CDs for electrochemical sensing

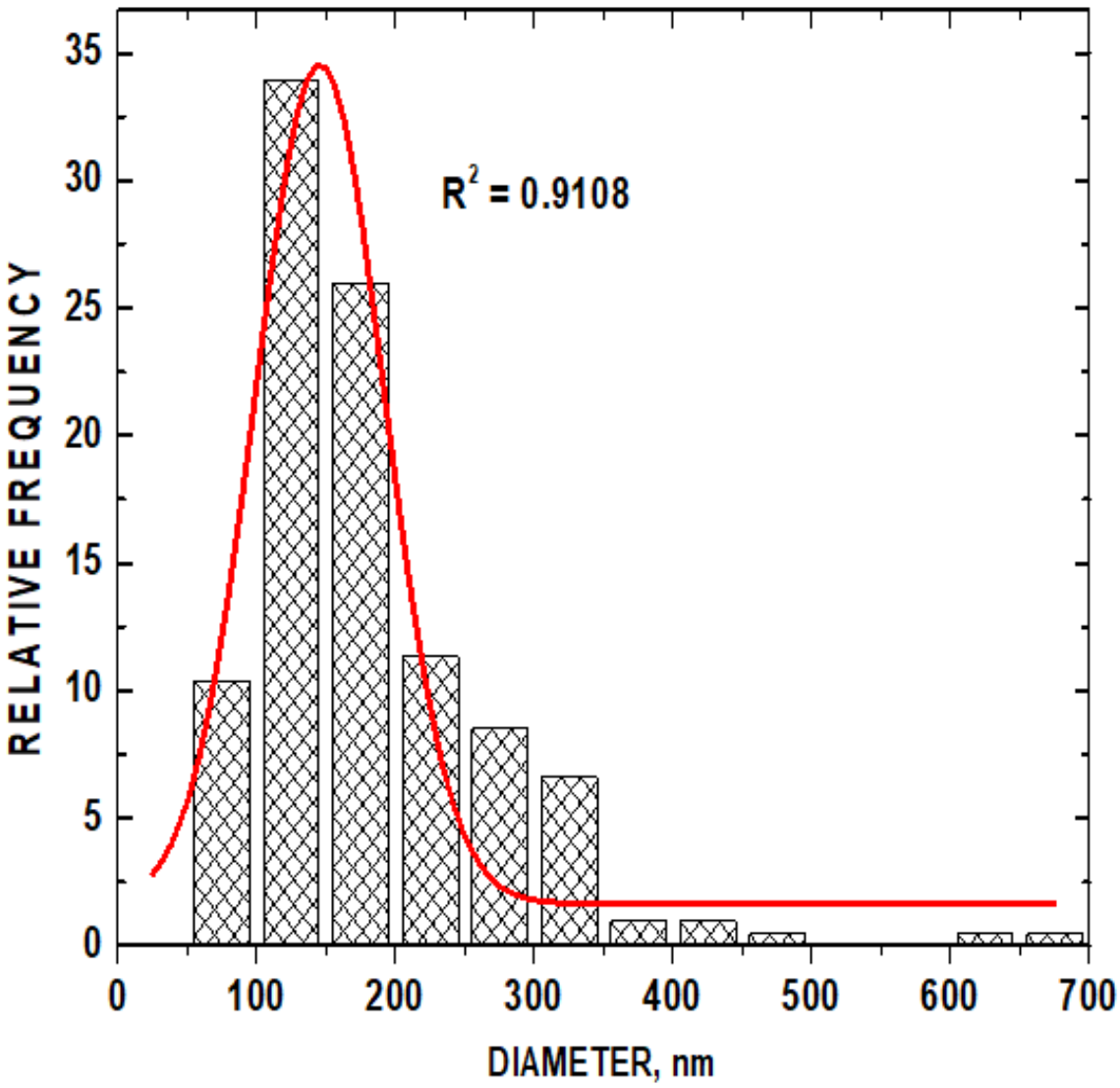

Fig. 20: Particle size distribution histogram of aggregated Lac CDs on the GCE surface

Raman spectroscopy

The defect densities of the GalCDs, LacCDs, and GluCDs are ranked in the following order based on Raman spectroscopy investigations conducted by Chusuei et al.: The GluCDs have the highest I_D/I_G ratio (0.153), followed by the LacCDs with a ratio of 0.108, and the GalCDs with a ratio of 0.0982.[53] Kislenko et al. identified that defects in graphene have the most significant impact on redox reactions that happen close to the Fermi level and have voltages between -0.2V and +0.3V.[54] The defects is due to the sp^3 hybridization which is seen as the D band in the raman spectra, the sp^2 Carbon entity gives the G-band. Introducing the defects in the graphene creates an electyron sink which enhance the conductivity and electron signal.

From my experiments, the dopamine detection was seen at an oxidation voltage of 0.25V, The graphene defect density predicts that GluCDs would have the highest electrochemical signal, but the experimental results show otherwise. The disparity from the expected results can be attributed to the existence of a significant accumulation of carbon dots, as evidenced by the scanning electron microscopy (SEM) data of the electrode surface. This agglomeration affects the extent to which faults are exposed to the dopamine analyte.

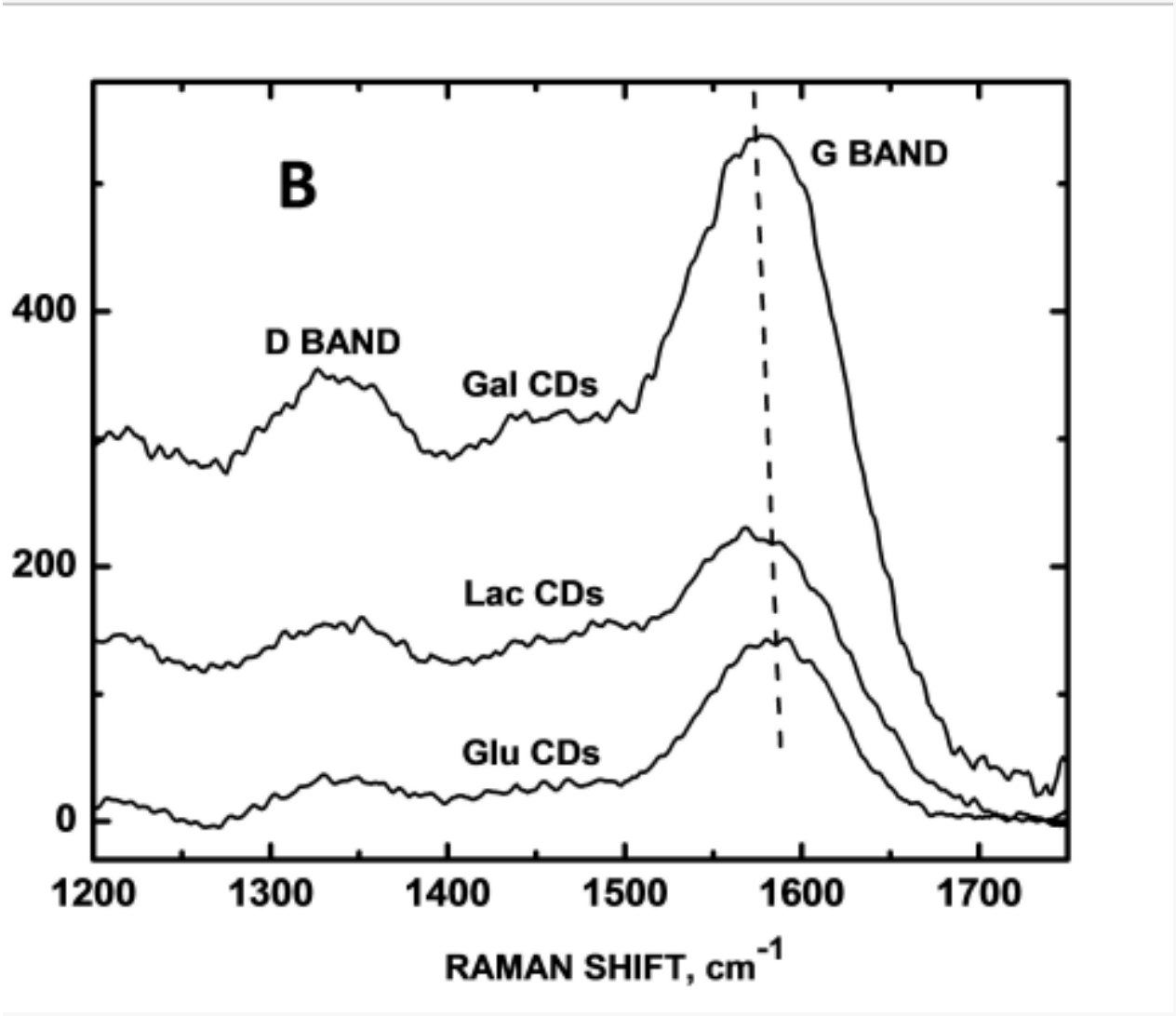

Fig. 21: Raman diamond bands of saccharide carbon dots.

CHAPTER IV

CONCLUSIONS

The main objective of this research is to develop an easily utilized test and analytical technique to detect dopamine, which is a common biomarker for neuroblastoma screening. Dr. Roger M. Leblanc, a renowned scientist associated with the Department of Chemistry at the University of Miami in Florida, prepared the carbon dots used in this study. They employed the method of hydrothermal synthesis. The developed saccharide glassy carbon electrode carbon dots showed sensitivity and selectivity towards the detection of dopamine; the sensitivity was studied by cyclic voltammetry experiments. The lactose carbon dots show the greatest sensitivity among the three carbon dots used, followed by glucose and then galactose carbon dots. The plot of peak current vs dopamine concentration at 0.01mM - 0.1mM and 0.1mM - 1mM shows a linear relationship, with the maximum current response found at the 1mM dopamine concentration. The plot of peak current from 0.01mM - 1mM dopamine concentration shows a fifth polynomial equation, which is a functional calibration plot with some constraints as a result of some solutions on the surface of the electrode. Uric acid and D-glucose were also biological compounds that may interfere with the neuroblastoma screening process, but they showed little or no response to the lactose carbon dots in the cyclic voltammetry experiment. Chronoamperometry experiment was also carried out to detect the lactose carbon dots selectivity towards dopamine, but there was no response.

A scanning electron microscope was used to analyze the surface morphology and distribution of the saccharide carbon dots on the surface of the glassy carbon electrode. The average sizes of the carbon dots were relatively uniform.

This result, along with the corresponding histogram, shows that the lactose carbon dots and glassy carbon electrode had excellent catalytic behavior towards the oxidation of dopamine. Also, the dopamine oxidation peak current was higher than that of other analytes (d-glucose and uric acid); this indicates that the lactose carbon dots can promote dopamine oxidation on the electrode surface due to their fast electron transfer capability and higher surface area.

Chusuei et al.'s Raman experiment revealed that glucose carbon dots have the highest ID/IG ratio, which indicates a higher density of graphene defects. In contrast, my results show that lactose carbon dots produce the highest electrochemical signal. This discrepancy can be better understood by considering the average size of the carbon dots, which are larger than the typical size (>10nm) measured using a scanning electron microscope. From my experiments, the dopamine detection was seen at an oxidation voltage of 0.25V, The graphene defect density predicts that GluCDs would have the highest electrochemical signal, but the experimental results show otherwise.

The disparity from the expected results can be attributed to the existence of a significant accumulation of carbon dots, as evidenced by the scanning electron microscopy (SEM) data of the electrode surface. This agglomeration affects the extent to which faults are exposed to the dopamine analyte.

REFERENCES

https://doi.org/10.1021/acs.langmuir.9b00920

(1) Konstantinova, E. A.; Le, N. T.; Kashkarov, P. K.; Zaytseva, A. A.; Kytin, V. G. Investigation of the Photoelectronic Properties of Nanocrystalline Carbon- and Nitrogen-Doped Titanium Dioxide. *Mosc. Univ. Phys. Bull.* **2014**, *69* (2), 180–184. https://doi.org/10.3103/S002713491402009X.

(2) Vollath, D. *Nanomaterials: An Introduction to Synthesis, Properties and Application*; Wiley-VCH: Weinheim, 2008.

(3) Badawi, A.; Al-Hosiny, N.; Abdallah, S.; Merazga, A.; Talaat, H. Single Wall Carbon Nanotube/Titania Nanocomposite Photoanodes Enhance the Photovoltaic Performance of Cadmium Selenide Quantum Dot-Sensitized Solar Cells. *Mater. Sci. Semicond. Process.* **2014**, *26*, 162–168. https://doi.org/10.1016/j.mssp.2014.04.028.

(4) Sarkar, K.; Sarkar, S.; Das, P. Kr. Spark Plasma Sintered Multiwalled Carbon Nanotube/Silicon Carbide Composites: Densification, Microstructure, and Tribo-Mechanical Characterization. *J. Mater. Sci.* **2016**, *51* (14), 6697–6710. https://doi.org/10.1007/s10853-016-9956-x.

(5) Ambrosi, A.; Pumera, M. Electrochemically Exfoliated Graphene and Graphene Oxide for Energy Storage and Electrochemistry Applications. *Chem. – Eur. J.* **2016**, *22* (1), 153–159. https://doi.org/10.1002/chem.201503110.

(6) Holá, K.; Pavliuk, M. V.; Németh, B.; Huang, P.; Zdražil, L.; Land, H.; Berggren, G.; Tian, H. Carbon Dots and [FeFe] Hydrogenase Biohybrid Assemblies for Efficient Light-Driven Hydrogen Evolution. *ACS Catal.* **2020**, *10* (17), 9943–9952. https://doi.org/10.1021/acscatal.0c02474.

(7) Xu, X.; Ray, R.; Gu, Y.; Ploehn, H. J.; Gearheart, L.; Raker, K.; Scrivens, W. A. Electrophoretic Analysis and Purification of Fluorescent Single-Walled Carbon Nanotube Fragments. *J. Am. Chem. Soc.* **2004**, *126* (40), 12736–12737. https://doi.org/10.1021/ja040082h.

(8) Singh, I.; Arora, R.; Dhiman, H.; Pahwa, R. Carbon Quantum Dots: Synthesis, Characterization and Biomedical Applications. *Turk. J. Pharm. Sci.* **2018**, *15* (2), 219–230. https://doi.org/10.4274/tjps.63497.

(9) Wang, Y.; Godin, R.; Durrant, J. R.; Tang, J. Efficient Hole Trapping in Carbon Dot/Oxygen-Modified Carbon Nitride Heterojunction Photocatalysts for Enhanced Methanol Production from CO_2 under Neutral Conditions. *Angew. Chem. Int. Ed.* **2021**, *60* (38), 20811–20816. https://doi.org/10.1002/anie.202105570.

(10) Rosso, C.; Filippini, G.; Prato, M. Carbon Dots as Nano-Organocatalysts for Synthetic Applications. *ACS Catal.* **2020**, *10* (15), 8090–8105. https://doi.org/10.1021/acscatal.0c01989.

(11) Seven, E. S.; Seven, Y. B.; Zhou, Y.; Poudel-Sharma, S.; Diaz-Rucco, J. J.; Kirbas Cilingir, E.; Mitchell, G. S.; Van Dyken, J. D.; Leblanc, R. M. Crossing the Blood–Brain Barrier with Carbon Dots: Uptake Mechanism and *in Vivo* Cargo Delivery. *Nanoscale Adv.* **2021**, *3* (13), 3942–3953. https://doi.org/10.1039/D1NA00145K.

(12) Dhenadhayalan, N.; Lin, K.; Saleh, T. A. Recent Advances in Functionalized Carbon Dots toward the Design of Efficient Materials for Sensing and Catalysis Applications. *Small* **2020**, *16* (1), 1905767. https://doi.org/10.1002/smll.201905767.

(13) Nunes, D.; Pimentel, A.; Pinto, J. V.; Calmeiro, T. R.; Nandy, S.; Barquinha, P.; Pereira, L.; Carvalho, P. A.; Fortunato, E.; Martins, R. Photocatalytic Behavior of TiO 2 Films Synthesized by Microwave Irradiation. *Catal. Today* **2016**, *278*, 262–270. https://doi.org/10.1016/j.cattod.2015.10.038.

(14) Yang, H.; Yang, L.; Yuan, Y.; Pan, S.; Yang, J.; Yan, J.; Zhang, H.; Sun, Q.; Hu, X. A Portable Synthesis of Water-Soluble Carbon Dots for Highly Sensitive and Selective Detection of Chlorogenic Acid Based on Inner Filter Effect. *Spectrochim. Acta. A. Mol. Biomol. Spectrosc.* **2018**, *189*, 139–146. https://doi.org/10.1016/j.saa.2017.07.065.

(15) Kim, M.; Osone, S.; Kim, T.; Higashi, H.; Seto, T. Synthesis of Nanoparticles by Laser Ablation: A Review. *KONA Powder Part. J.* **2017**, *34* (0), 80–90. https://doi.org/10.14356/kona.2017009.

(16) Reyes, D.; Camacho, M.; Camacho, M.; Mayorga, M.; Weathers, D.; Salamo, G.; Wang, Z.; Neogi, A. Laser Ablated Carbon Nanodots for Light Emission. *Nanoscale Res. Lett.* **2016**, *11* (1), 424. https://doi.org/10.1186/s11671-016-1638-8.

(17) Kaczmarek, A.; Hoffman, J.; Morgiel, J.; Mościcki, T.; Stobiński, L.; Szymański, Z.; Małolepszy, A. Luminescent Carbon Dots Synthesized by the Laser Ablation of Graphite in Polyethylenimine and Ethylenediamine. *Materials* **2021**, *14* (4), 729. https://doi.org/10.3390/ma14040729.

(18) Chao-Mujica, F. J.; Garcia-Hernández, L.; Camacho-López, S.; Camacho-López, M.; Camacho-López, M. A.; Reyes Contreras, D.; Pérez-Rodríguez, A.; Peña-Caravaca, J. P.; Páez-Rodríguez, A.; Darias-Gonzalez, J. G.; Hernandez-Tabares, L.; Arias De Fuentes, O.; Prokhorov, E.; Torres-Figueredo, N.; Reguera, E.; Desdin-García, L. F. Carbon Quantum Dots by Submerged Arc Discharge in Water: Synthesis, Characterization, and Mechanism of Formation. *J. Appl. Phys.* **2021**, *129* (16), 163301. https://doi.org/10.1063/5.0040322.

(19) Jiang, Y.; Wei, G.; Zhang, W.; Wang, Z.; Cheng, Y.; Dai, Z. Solid Phase Reaction Method for Preparation of Carbon Dots and Multi-Purpose Applications. *Sens. Actuators B Chem.* **2016**, *234*, 15–20. https://doi.org/10.1016/j.snb.2016.04.124.

(20) Li, X.; Ge, F.; Li, X.; Zhou, X.; Qian, J.; Fu, G.; Shi, L.; Xu, Y. Rapid and Large-Scale Production of Carbon Dots by Salt-Assisted Electrochemical Exfoliation of Graphite Rods. *J. Electroanal. Chem*. **2019**, *851*, 113390. https://doi.org/10.1016/j.jelechem.2019.113390.

(21) Zhou, S.; Guo, P.; Li, J.; Meng, L.; Gao, H.; Yuan, X.; Wu, D. An Electrochemical Method for Evaluation the Cytotoxicity of Fluorene on Reduced Graphene Oxide Quantum Dots Modified Electrode. *Sens. Actuators B Chem*. **2018**, *255*, 2595–2600. https://doi.org/10.1016/j.snb.2017.09.066.

(22) Sakdaronnarong, C.; Sangjan, A.; Boonsith, S.; Kim, D. C.; Shin, H. S. Recent Developments in Synthesis and Photocatalytic Applications of Carbon Dots. *Catalysts* **2020**, *10* (3), 320. https://doi.org/10.3390/catal10030320.

(23) Huo, Y.; Xiu, S.; Meng, L.-Y.; Quan, B. Solvothermal Synthesis and Applications of Micro/Nano Carbons: A Review. *Chem. Eng. J.* **2023**, *451*, 138572. https://doi.org/10.1016/j.cej.2022.138572.

(24) Hallaji, Z.; Bagheri, Z.; Ranjbar, B. One-Step Solvothermal Synthesis of Red Chiral Carbon Dots for Multioptical Detection of Water in Organic Solvents. *ACS Appl. Nano Mater.* **2023**, *6* (5), 3202–3210. https://doi.org/10.1021/acsanm.2c04466.

(25) Hebbar, A.; Selvaraj, R.; Vinayagam, R.; Varadavenkatesan, T.; Kumar, P. S.; Duc, P. A.; Rangasamy, G. A Critical Review on the Environmental Applications of Carbon Dots. *Chemosphere* **2023**, *313*, 137308. https://doi.org/10.1016/j.chemosphere.2022.137308.

(26) Nammahachak, N.; Aup-Ngoen, K. K.; Asanithi, P.; Horpratum, M.; Chuangchote, S.; Ratanaphan, S.; Surareungchai, W. Hydrothermal Synthesis of Carbon Quantum Dots with Size Tunability *via* Heterogeneous Nucleation. *RSC Adv.* **2022**, *12* (49), 31729–31733. https://doi.org/10.1039/D2RA05989D.

(27) Yang, Z.-C.; Wang, M.; Yong, A. M.; Wong, S. Y.; Zhang, X.-H.; Tan, H.; Chang, A. Y.; Li, X.; Wang, J. Intrinsically Fluorescent Carbon Dots with Tunable Emission Derived from Hydrothermal Treatment of Glucose in the Presence of Monopotassium Phosphate. *Chem. Commun.* **2011**, *47* (42), 11615. https://doi.org/10.1039/c1cc14860e.

(28) Sadhanala, H. K.; Khatei, J.; Nanda, K. K. Facile Hydrothermal Synthesis of Carbon Nanoparticles and Possible Application as White Light Phosphors and Catalysts for the Reduction of Nitrophenol. *RSC Adv.* **2014**, *4* (22), 11481. https://doi.org/10.1039/c3ra47527a.

(29) Kamano, Y.; Kadota, K.; Shimosaka, A.; Shirakawa, Y.; Hidaka, J. Quantitative Evaluation on the Heterogeneous Nucleation of Amino Acid by a Thermodynamic Analysis. *J. Mol. Liq.* **2014**, *200*, 474–479. https://doi.org/10.1016/j.molliq.2014.11.021.

(30) Liu, G.; Li, S.; Cheng, M.; Zhao, L.; Zhang, B.; Gao, Y.; Xu, Y.; Liu, F.; Lu, G. Facile Synthesis of Nitrogen and Sulfur Co-Doped Carbon Dots for Multiple Sensing Capacities: Alkaline Fluorescence Enhancement Effect, Temperature Sensing, and Selective Detection of Fe^{3+} Ions. *New J. Chem.* **2018**, *42* (15), 13147–13156. https://doi.org/10.1039/C8NJ02086H.

(31) Huang, G.; Lu, C.-H.; Yang, H.-H. Magnetic Nanomaterials for Magnetic Bioanalysis. In *Novel Nanomaterials for Biomedical, Environmental and Energy Applications*; Elsevier, 2019; pp 89–109. https://doi.org/10.1016/B978-0-12-814497-8.00003-5.

(32) Qiu, J.; Li, Y.; Jia, Y. Synthesis Methods. In *Persistent Phosphors*; Elsevier, 2021; pp 31–67. https://doi.org/10.1016/B978-0-12-818637-4.00002-1.

(33) Swift, C. C.; Eklund, M. J.; Kraveka, J. M.; Alazraki, A. L. Updates in Diagnosis, Management, and Treatment of Neuroblastoma. *RadioGraphics* **2018**, *38* (2), 566–580. https://doi.org/10.1148/rg.2018170132.

(34) Strenger, V.; Kerbl, R.; Dornbusch, H. J.; Ladenstein, R.; Ambros, P. F.; Ambros, I. M.; Urban, C. Diagnostic and Prognostic Impact of Urinary Catecholamines in Neuroblastoma Patients. *Pediatr. Blood Cancer* **2007**, *48* (5), 504–509. https://doi.org/10.1002/pbc.20888.

(35) Youngblood, J. Neuroblastoma: Sonography's Major Role in Its Diagnosis and Treatment. *J. Diagn. Med. Sonogr.* **2012**, *28* (2), 58–65. https://doi.org/10.1177/8756479312439624.

(36) Zhang, Y.; Liu, F.; Xiao, F.; Wu, Q. Effects of an Ingredient of Bupleurum On Dopamine D2 Receptor-Mediated Signaling in Human Neuroblastoma Cell Line. *Eur. Psychiatry* **2015**, *30*, 1617. https://doi.org/10.1016/S0924-9338(15)31249-9.

(37) Xie, L.; Liu, Y.; Zhang, W.; Xu, S. A Dopamine/Tannic-Acid-Based Co-Deposition Combined with Phytic Acid Modification to Enhance the Anti-Fouling Property of RO Membrane. *Membranes* **2021**, *11* (5), 342. https://doi.org/10.3390/membranes11050342.

(38) Fan, B.; Zhu, Y.; Rechenberg, R.; Becker, M. F.; Li, W. A FLEXIBLE, LARGE-SCALE DIAMOND-POLYMER CHEMICAL SENSOR FOR NEUROTRANSMITTER DETECTION. In *2016 Solid-State, Actuators, and Microsystems Workshop Technical Digest*; Transducer Research Foundation: Hilton Head, South Carolina, USA, 2016; pp 320–323. https://doi.org/10.31438/trf.hh2016.87.

(39) Zhang, X.; Li, G.; Chen, G.; Wu, D.; Wu, Y.; James, T. D. Enzyme Mimics for Engineered Biomimetic Cascade Nanoreactors: Mechanism, Applications, and Prospects. *Adv. Funct. Mater.* **2021**, *31* (50), 2106139. https://doi.org/10.1002/adfm.202106139.

(40) Kissinger, P. T.; Heineman, W. R. Cyclic Voltammetry. *J. Chem. Educ.* **1983**, *60* (9), 702. https://doi.org/10.1021/ed060p702.

(41) Mizher Radhi, M.; Ali Mossa, A.; Abbas Jaffar Al-Mulla, E.; Naeemah Lafta, A. Electrochemical Study of Modified Glassy Carbon Electrode with Polyaniline Nanoparticles Using Cyclic

Voltammetry. *Bull. Chem. Soc. Ethiop.* **2022**, *36* (3), 687–696. https://doi.org/10.4314/bcse.v36i3.17.

(42) Horwood, C. Ionic Liquids as Electrolytes for Electrochemistry. In *Ionic Liquids in Analytical Chemistry*; Elsevier, 2022; pp 329–342. https://doi.org/10.1016/B978-0-12-823334-4.00012-6.

(43) Shao, H.; Wu, D.; Li, Y.; Liu, W.; Chu, X. Improved Signal-to-noise Ratio Estimation Algorithm for Asymmetric Pulse-shaped Signals. *IET Commun.* **2015**, *9* (14), 1788–1792. https://doi.org/10.1049/iet-com.2014.1162.

(44) Marabotti, P.; Peggiani, S.; Facibeni, A.; Serafini, P.; Milani, A.; Russo, V.; Li Bassi, A.; Casari, C. S. In Situ Surface-Enhanced Raman Spectroscopy to Investigate Polyyne Formation during Pulsed Laser Ablation in Liquid. *Carbon* **2022**, *189*, 219–229. https://doi.org/10.1016/j.carbon.2021.12.060.

(45) Lee, J. B.; Lee, D. R.; Choi, N. C.; Jang, J.; Park, C. H.; Yoon, M. S.; Lee, M.; Won, K.; Hwang, J. S.; Kim, B. M. Efficient Dermal Delivery of Retinyl Palmitate: Progressive Polarimetry and Raman Spectroscopy to Evaluate the Structure and Efficacy. *Eur. J. Pharm. Sci. Off. J. Eur. Fed. Pharm. Sci.* **2015**, *78*, 111–120. https://doi.org/10.1016/j.ejps.2015.07.009.

(46) Hoskins, L. C. Pure Rotational Raman Spectroscopy: A Dry-Lab Experiment. *J. Chem. Educ.* **1977**, *54* (10), 642. https://doi.org/10.1021/ed054p642.

(47) Wang, H.; Ma, F.; Wang, F.; Liu, D.; Li, X.; Du, S. Identification of Motor and Sensory Fascicles in Peripheral Nerve Trunk Using Immunohistochemistry and Micro-Raman Spectroscopy. *J. Trauma Inj. Infect. Crit. Care* **2011**, *71* (5), 1246–1251. https://doi.org/10.1097/TA.0b013e31822503a7.

(48) Marshall, A. G.; Damo, S. M.; Hinton, A. Revisiting Focused Ion Beam Scanning Electron Microscopy. *Trends Biochem. Sci.* **2023**, *48* (6), 585–586. https://doi.org/10.1016/j.tibs.2023.02.005.

(49) Parisi, L.; Toffoli, A.; Ghezzi, B.; Lagonegro, P.; Trevisi, G.; Macaluso, G. M. Preparation of Hybrid Samples for Scanning Electron Microscopy (SEM) Coupled to Focused Ion Beam (FIB) Analysis: A New Way to Study Cell Adhesion to Titanium Implant Surfaces. *PLOS ONE* **2022**, *17* (8), e0272486. https://doi.org/10.1371/journal.pone.0272486.

(50) Heymann, J. A. W.; Shi, D.; Kim, S.; Bliss, D.; Milne, J. L. S.; Subramaniam, S. 3D Imaging of Mammalian Cells with Ion-Abrasion Scanning Electron Microscopy. *J. Struct. Biol.* **2009**, *166* (1), 1–7. https://doi.org/10.1016/j.jsb.2008.11.005.

(51) Ohnsorge, J.; Holm, R. *Rasterelektronenmikroskopie: eine Einführung für Mediziner und Biologen = Scanning electron microscopy*; Thieme: Stuttgart, 1973.

(52) Seven, E. S.; Sharma, S. K.; Meziane, D.; Zhou, Y.; Mintz, K. J.; Pandey, R. R.; Chusuei, C. C.; Leblanc, R. M. Close-Packed Langmuir Monolayers of Saccharide-Based Carbon Dots at the Air–Subphase Interface. *Langmuir* **2019**, *35* (20), 6708–6718. https://doi.org/10.1021/acs.langmuir.9b00920.

(53) Chusuei, C. C.; Clark, C. J.; Pandey, R. R.; Williams, E. T.; Shuxteau, C.; Seven, E. S.; Leblanc, R. M. Graphene Defects in Saccharide Carbon Dots Govern Electrochemical Sensitivity. *Electroanalysis* **2021**, *33* (11), 2261–2266. https://doi.org/10.1002/elan.202100381.

(54) Kislenko, V. A.; Pavlov, S. V.; Kislenko, S. A. Influence of Defects in Graphene on Electron Transfer Kinetics: The Role of the Surface Electronic Structure. *Electrochimica Acta* **2020**, *341*, 136011. https://doi.org/10.1016/j.electacta.2020.136011.

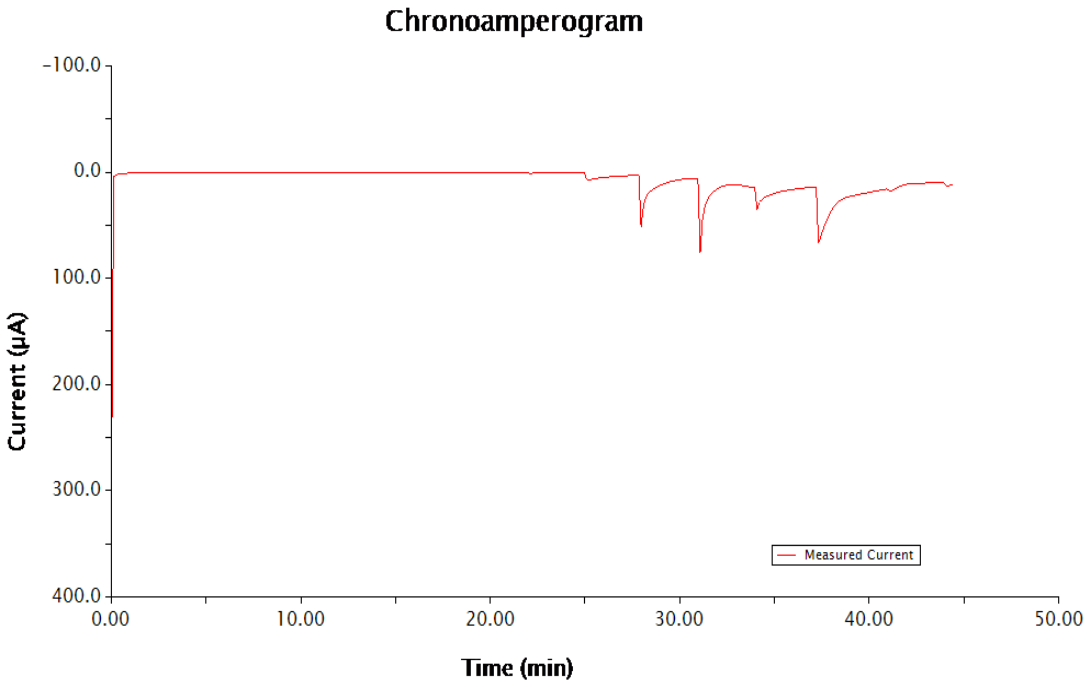

Fig 22: Chronoamperometry response of lactose carbon dots towards increasing concentration of dopamine.

CCC Marketplace

Order Number: 1414037
Order Date: 07 Nov 2023

Payment Information

Peter Ogunsanya
opo2c@mtmail.mtsu.edu
Payment method: Invoice

Billing Address:
Peter Ogunsanya
Middle Tennessee State Univers
ity
5350 cane ridge road
Antioch, TN 37013
United States

+1 (931) 237-3065
opo2c@mtmail.mtsu.edu

Customer Location:
Peter Ogunsanya
Middle Tennessee State Univers
ity
5350 cane ridge road
Antioch, TN 37013
United States

Order Details

1. Electroanalysis

Billing Status: Open

Article: Graphene Defects in Saccharide Carbon Dots Govern Electrochemical Sensitivity

Order License ID	1414037-1	**Type of Use**	Republish in a thesis/dissertation
Order detail status	Completed		
ISSN	1040-0397	**Publisher**	WILEY - V C H VERLAG GMBH & CO. KGAA
		Portion	Image/photo/illustration

0.00 USD
Republication Permission

LICENSED CONTENT

Publication Title	Electroanalysis	**Rightsholder**	John Wiley & Sons - Books
Article Title	Graphene Defects in Saccharide Carbon Dots Govern Electrochemical Sensitivity	**Publication Type**	Journal
		Start Page	2261
		End Page	2266
Author/Editor	Wang, Joseph	**Issue**	11
Date	01/01/1989	**Volume**	33
Language	English		
Country	Germany		

REQUEST DETAILS

Portion Type	Image/photo/illustration	**Distribution**	Worldwide
Number of Images / Photos / Illustrations	1	**Translation**	Original language of publication
Format (select all that apply)	Print, Electronic	**Copies for the Disabled?**	No
		Minor Editing Privileges?	No
Who Will Republish the Content?	Academic institution	**Incidental Promotional Use?**	No
Duration of Use	Life of current and all future editions	**Currency**	USD
Lifetime Unit Quantity	Up to 499		
Rights Requested	Main product		

NEW WORK DETAILS

Title	Assaying Dopamine HCl with Saccharide Carbon Dots	**Institution Name**	Middle Tennessee State University
Instructor Name	Peter Ogunsanya	**Expected Presentation Date**	2023-12-01

ADDITIONAL DETAILS

The Requesting Person / Organization to Appear on the License Peter Ogunsanya

REQUESTED CONTENT DETAILS

Title, Description or Numeric Reference of the Portion(s)	Raman diamond bands of saccharide CDs	**Title of the Article / Chapter the Portion Is From**	Graphene Defects in Saccharide Carbon Dots Govern Electrochemical Sensitivity
Editor of Portion(s)	Chusuei, Charles C.; Clark, Christopher J.; Pandey, Raja Ram; Williams, Ethan T.; Shuxteau, Carissa; Seven, Elif	**Author of Portion(s)**	Chusuei, Charles C.; Clark, Christopher J.; Pandey, Raja Ram; Williams, Ethan T.; S.; Leblanc, Roger M. Shuxteau, S.; Leblanc, Roger M.
Volume / Edition	33		
		Publication Date of Portion	2021-11-11
Page or Page Range of Portion	2261-2266		

John Wiley & Sons - Books Terms and Conditions

No right, license or interest to any trademark, trade name, service mark or other branding ("Marks") of WILEY or its licensors is granted hereunder, and you agree that you shall not assert any such right, license or interest with respect thereto. You may not alter, remove or suppress in any manner any copyright, trademark or other notices displayed by the Wiley material. This Agreement will be void if the Type of Use, Format, Circulation, or Requestor Type was misrepresented during the licensing process. In no instance may the total amount of Wiley Materials used in any Main Product, Compilation or Collective work comprise more than 5% (figures/tables) or 15% (if full articles/chapters) of the (entirety of the) Main Product, Compilation or Collective Work. Some titles may be available under an Open Access license. It is the Licensors' responsibility to identify the type of Open Access license on which the requested material was published, and comply fully with the terms of that license for the type of use specified Further details can be found on Wiley Online Library http://olabout.wiley.com/WileyCDA/Section/id-410895.html.

Total Items: 1 Subtotal: 0.00

USD

Order Total: 0.00

USD

Marketplace Permissions General Terms and Conditions

The following terms and conditions ("General Terms"), together with any applicable Publisher Terms and Conditions, govern User's use of Works pursuant to the Licenses granted by Copyright Clearance Center, Inc. ("CCC") on behalf of the applicable Rightsholders of such Works through CCC's applicable Marketplace transactional licensing services (each, a "Service").

1) **Definitions.** For purposes of these General Terms, the following definitions apply:

"License" is the licensed use the User obtains via the Marketplace platform in a particular licensing transaction, as set forth in the Order Confirmation.

"Order Con rmation" is the con rmation CCC provides to the User at the conclusion of each Marketplace transaction. "Order Con rmation Terms" are additional terms set forth on speci c Order Con rmations not set forth in the General Terms that can include terms applicable to a particular CCC transactional licensing service and/or any Rightsholder-speci c terms.

"Rightsholder(s)" are the holders of copyright rights in the Works for which a User obtains licenses via the Marketplace platf orm, which are displayed on speci c Order Con rmations.

"Terms" means the terms and conditions set forth in these General Terms and any additional Order Con rmation Terms collectively.

"User" or "you" is the person or entity making the use granted under the relevant License. Where the person accepting the Terms on behalf of a User is a freelancer or other third party who the User authorized to accept the General Terms on the User's behalf, such person shall be deemed jointly a User for purposes of such Terms.

ELSEVIER LICENSE

TERMS AND CONDITIONS

Dec 01, 2023

This Agreement between Middle Tennessee State University -- Peter Ogunsanya ("You") and Elsevier ("Elsevier") consists of your license details and the terms and conditions provided by Elsevier and Copyright Clearance Center.

License Number	5660390049910
License date	Nov 01, 2023
Licensed Content Publisher	Elsevier
Licensed Content Publication	Chemosphere
Licensed Content Title	A critical review on the environmental applications of carbon dots
Licensed Content Author	Akshatha Hebbar,Raja Selvaraj,Ramesh Vinayagam,Thivaharan Varadavenkatesan,Ponnusamy Senthil Kumar,Pham Anh Duc,Gayathri Rangasamy
Licensed Content Date	Feb 1, 2023

Licensed Content Volume	313
Licensed Content Issue	n/a
Licensed Content Pages	1
Start Page	137308
End Page	0
Type of Use	reuse in a thesis/dissertation
Portion	figures/tables/illustrations
Number of figures/tables/illustrations	1
Format	both print and electronic
Are you the author of this Elsevier article?	No
Will you be translating?	No
Title of new work	Assaying dopamine HCl with saccharide carbon dots
Institution name	Middle Tennessee State University
Expected presentation date	Dec 2023
Portions	Figure 2

Requestor Location	Middle Tennessee State University 5350 cane ridge road ANTIOCH, TN 37013 United States Attn: Middle Tennessee State University
Publisher Tax ID	98-0397604
Total	0.00 USD

Terms and Conditions

INTRODUCTION